Multiple zebrafish *atoh1* genes specify a diversity of neuronal types in the zebrafish hindbrain

Chelsea U. Kidwell

A dissertation

submitted in partial fulfillment of the

requirements for the degree of

Doctor of Philosophy

University of Washington

2016

Reading Committee:

Cecilia Moens, Chair

David Parichy

Jay Parrish

Program Authorized to Offer Degree:

Biology

University of Washington

Abstract

Multiple zebrafish *atoh1* genes specify a diversity of neuronal types in the zebrafish hindbrain

Chelsea U. Kidwell

Chair of the Supervisory Committee:

Affiliate Professor Cecilia B. Moens

Department of Biology

The basic Helix-Loop-Helix transcription factor, Atoh1, is known to specify several neuronal subtypes including one of most abundant cell types in the vertebrate brain, cerebellar granule neurons. The function of *atoh1* in the development of cerebellar granule neurons is poorly understood. Here we use the zebrafish CNS to explore the role of *atoh1* in granule neuron specification and in the generation of neuronal diversity. With the use of single and compound *atoh1* mutants, we show that out of the three *atoh1* genes in the zebrafish genome, *atoh1c* plays the most prominent role in granule neuron development but together *atoh1c* and *atoh1a* are required for the full complement of granule neurons. Interestingly, *atoh1a* and *atoh1c* specify non-overlapping granule populations, indicating that fish use multiple *atoh1* genes to generate

additional neuronal diversity that is not detected in mammals. In addition, we have identified a novel population of *atoh1c*-derived neurons closely associated with the conserved noradrenergic neurons of the Locus Coeruleus. Finally, with the use of live imaging possible in zebrafish, we discovered expression of *atoh1c* at the rhombic lip promotes the apical detachment of granule neuron progenitors from surrounding neuroepithelium and this process is critical for neuronal maturation. This study provides us with a better understanding of how a proneural transcription factor influences neurogenesis in the vertebrate brain.

Table of Contents

List of Figures

Acknowledgments

First, I would like to thank Cecilia for giving me the opportunity to be a part of her lab. I feel extremely lucky to have learned from such an outstanding scientist who is someone that always leads by example. Cecilia, you have been unwavering in your support and have gone above and beyond to help me achieve my goals, I am truly grateful to have had you to guide me along the way. To Chen-Ying Su, Luyuan Pan, Adam Miller, and Minna Roh-Johnson: thank you for serving as amazing mentors during my graduate career. By working alongside each one of you, I have learned how great scientists learn, think, act, and work. To Chen-Ying: thank you for your contribution to the work presented in this dissertation. To all other Moens lab members: thank you for making the Moens lab an exceptional place to work. Thank you to Gabby for her encouragement and for serving as an overflowing source of optimism. To Rachel, Arish, and Jason: thank you for your technical support.

I would like to thank all of the members of my thesis committee for their support. Thank you to David Parichy, Jay Parish, and Cecilia Moens for the careful reading of this dissertation.

I thank the Developmental Biology Training Grant for funding and training. Thank you to David Raible, the training grant director, for his sponsorship during my time on the grant.

To my family and friends: thank you for your constant encouragement and love, it means the world to me. To my mom, thank you for being my biggest supporter. It is because of you, that I am able to and will continue to persevere through challenging times in my life. To Chris: thank you for supporting me in every way possible. I am so grateful to have you as my partner in life. Last but not least, to Elias, thank you for lifting me up with your infectious spirit and loving smile.

Chapter 1: Introduction

Dissecting the genetic programs that underlie the production of neuronal diversity is key to understanding the function of circuits that make up the complex vertebrate brain. The generation of diverse neuronal cell types begins in the neural tube of the early embryo. Global signaling networks allow the neural tissue to acquire spatial information, from there neurogenesis begins with the expression of basic-Helix-Loop-Helix (bHLH) transcription factors that define the eventual fate of the expressing cells. The spatiotemporal distribution of these transcription factors demarcates progenitor domains that will produce many neuron subtypes that serve a range of functions throughout the central nervous system (CNS). Here we explore the neuronal diversity generated by the *atonal(atoh)1* gene family.

***atonal*: Proneural Gene in Fly**

atonal family genes encode a conserved family of bHLH transcription factors well-known for their roles in the specification of sensory and neuronal cell types in all animals (Bertrand et al., 2002). Atonal was first described in the fly where it was found to be expressed during early development in the peripheral nervous system, the eye disc, and in the brain lobe (Jarman et al., 1993) and subsequently shown to be required for the formation of chordotonal organs, internal stretch and vibration receptors (Jarman et al., 1993), and photoreceptors in the eye (Jarman et al., 1994; Jarman et al., 1995). Through loss- and gain-of-function studies as well as analysis of expression patterns, it was determined that Atonal was necessary for the acquisition of neural, rather than epidermal, identity from a relatively equipotent field of ectodermal cells, a function termed proneural (Jarman et al., 1993; Jarman et al., 1994; Jarman et al., 1995).

***math1*: mouse atonal homolog 1**

Shortly after the discovery of *atonal* in fly, homologues in other animals were described (Ben-Arie et al., 1996). Math1 (mouse atonal homolog 1; herein referred to as *atoh1*) is the closest related homolog in mouse sharing ~70% identity with *atonal* in the bHLH domain (Akazawa et al., 1995) and is expressed in the CNS, the inner ear, and sensory cell types. Here I will focus on Atoh1 in the CNS.

Expression of *atoh1* begins at 9.5 dpc (days post conception) in the dorsal neural tube where its highest levels are detected in the cerebellum, pons, and medulla (Akazawa et al., 1995; Ben-Arie et al., 2000; Ben-Arie et al., 1996; Machold and Fishell, 2005; Rose et al., 2009a; Rose et al., 2009b; Wang et al., 2005). This broad expression is slowly restricted over time and by 19 dpc, *atoh1* is primarily detected in the cerebellum, in a region referred to as the external granule layer (EGL) where granule neurons are born and proliferate (Akazawa et al., 1995; Ben-Arie et al., 1997; Ben-Arie et al., 1996; Machold and Fishell, 2005; Rose et al., 2009a; Wang et al., 2005). Genetic lineage tracing in the mouse has demonstrated that *atoh1*-expressing progenitors give rise to diverse neuron types in the anterior hindbrain including ~9 tegmental neuron groups, deep cerebellar output neurons, and cerebellar granule neurons (Akazawa et al., 1995; Ben-Arie et al., 1997; Ben-Arie et al., 2000; Bermingham et al., 2001; Englund et al., 2006; Gray, 2008; Green et al., 2014; Machold and Fishell, 2005; Rose et al., 2009a; Wang et al., 2005; Wingate and Hatten, 1999). Functional studies on Atoh1 has demonstrated its requirement in the specification of many of the neuronal cell types listed above including cerebellar granule neurons (Ben-Arie et al., 1997; Bermingham et al., 1999; Bermingham et al., 2001; Rose et al., 2009a;

Rose et al., 2009b). Next, I will describe anterior most region of the hindbrain, the cerebellum, and what is known about the role of Atoh1 in this region.

The Cerebellum

The cerebellum is well known for its importance in motor coordination necessary for the generation of smooth and skillful movements (Leto et al., 2015). The relatively simple nature and stereotyped cytoarchitecture of the cerebellar circuit has made it an excellent model to study neurogenesis. In all vertebrates, the cerebellum is composed of excitatory glutamatergic granule neurons and the inhibitory GABAergic Purkinje neurons organized into a three-layered structure consisting of a superficial molecular layer, an underlying Purkinje layer, and a deep granule neuron layer (Fig. 1) (Butts et al., 2014; Hashimoto and Hibi, 2012; Leto et al., 2015). During development, cerebellar neurons are born in germinal zones within the dorso-anterior hindbrain: granule neuron progenitors in the upper rhombic lip (URL) and Purkinje neurons in the adjacent ventricular zone. Granule neuron progenitors migrate tangentially from the URL across the surface of the presumptive cerebellum and transiently reside in the EGL, where they undergo massive proliferation. From the EGL, they radially migrate inward to form the internal granule layer (IGL) and subsequently send their well-defined axons, parallel fibers, into the molecular layer where they synapse with the axons of neurons in the Purkinje layer (Fig. 1) (Leto et al., 2015).

atoh1 has been shown to be essential for the generation of granule neurons. Mice mutant for *atoh1* have a complete loss of the EGL as well as granule neurons resulting in a disorganization of the cerebellar structure (Ben-Arie et al., 1997; Ben-Arie et al., 2000). The functional and behavioral consequences of this phenotype have not been evaluated due to the fact

that *atoh1*$^{-/-}$ mice die shortly after birth from respiratory failure unrelated to the cerebellar defects (Ben-Arie et al., 1997). With the use of an *atoh1* transgenic reporter, Ben-Arie et al. show a loss of proliferation and migration of the *atoh*$^{-/-}$ granule progenitors out of the URL and speculate this phenotype is due to either the lack of granule neuron precursors or the inability of the population to proliferate and/or differentiate (Ben-Arie et al., 1997; Ben-Arie et al., 2000). The underlying cell biology of this phenotype has not been investigated further and therefore we sought to understand more about the developmental program underlying granule neuron specification using the zebrafish cerebellum as our model.

Zebrafish *atoh1* Genes and Cerebellum

Zebrafish have three *atoh1* genes: *atoh1a*, *1b*, and *1c,* all of which are expressed in overlapping but distinct progenitor domains within the rhombic lip of the hindbrain. Initial studies have described the expression of the three zebrafish *atoh1* genes (Chaplin et al., 2010; Kani et al., 2010) but their function in cerebellar development has yet to be explored.

The Corpus Cerebelli (CCe) of the fish cerebellum is homologous to the mammalian cerebellar vermis and is thought to be involved with autonomic functions such as respiration as well as emotion associated learning such as fear conditioning (Matsui et al., 2014). Its granule neurons elaborate axons that bifurcate in the molecular layer to form parallel fibers that synapse with Purkinje neuron axons in the canonical three-layer organization described above (Fig. 1) (Bae et al., 2009; Takeuchi et al., 2015a). Fish lack the massive expansion of granule neuron precursors that drive the formation of the foliated cerebellar hemispheres in mammals (Altman and Bayer, 1997), but have other unique cerebellar domains: the anterior-most Valvula (Va) which contains granule neuron progenitors that persist throughout adult life (Kani et al., 2010;

Kaslin et al., 2009), while the lateral eminentia granularis (EG) and the caudal Lobus Caudalis (LCa) control motor coordination in response to vestibular information (See schematic in figure 2) (Volkmann et al., 2008). The EG and LCa only contain granule neurons which protect parallel fibers both within as well as out of the cerebellum to a cerebellar-like structure, the cerebellar crest, in the hindbrain (Bae et al., 2009; Takeuchi et al., 2015b). The granule neurons in all cerebellar regions, as in other vertebrates, originate at the URL, as do some tegmental neurons and Eurydendroid cells, the equivalent of deep cerebellar output neurons (Fig. 1) (Kani et al., 2010; Volkmann et al., 2010). How the URL generates these many different cell types is not known in any system.

We sought to discover the role of zebrafish *atoh1* genes in the generation of neuronal diversity in the cerebellum, and to take advantage of the live imaging possible in zebrafish to study how *atoh1* genes control cerebellar progenitor migration and differentiation at high spatial and temporal resolution. Using single and compound mutants we describe a predominant role for *atoh1c* and a lesser role for *atoh1a* in the specification of cerebellar granule neurons in zebrafish. Using long-lived *atoh1a* and *atoh1c* reporters to follow their derivatives through larval development, we find that *atoh1a* and *atoh1c* specify non-overlapping granule and tegmental populations, indicating that fish use multiple *atoh1* genes rather than using a single *atoh1* gene over an extended developmental time to generate neuronal diversity. By live imaging, we show that *atoh1c* expression at the rhombic lip is required not for cell cycle exit or initial neuronal differentiation but for granule neuron progenitors to release their epithelial contacts and migrate away from the URL.

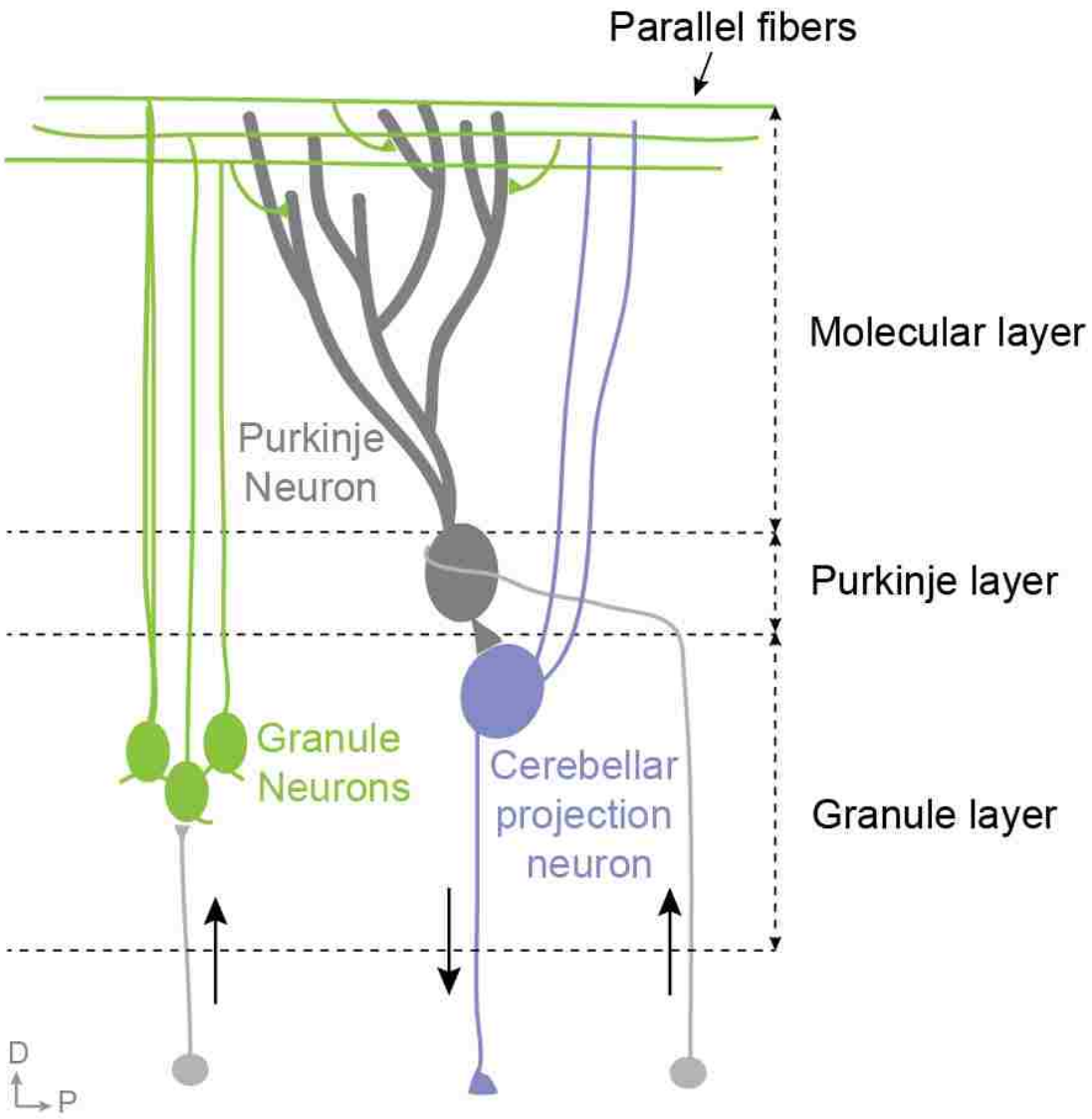

Figure 1. The mature cerebellar circuit.

Schematic of cross section through a mature vertebrate cerebellum. The three-layered structure of the cerebellum consists of (from superficial to deep) a molecular layer, Purkinje layer, and granule layer. The two primary cerebellar cell types are the granule neurons (green) and the Purkinje neurons (dark gray). Projection neurons are the output neuron of the cerebellum (purple). D: dorsal, P: posterior.

Chapter 2: Materials and Methods

Ethics statement

Experiments using zebrafish (*Danio rerio)* followed the Fred Hutchinson Cancer Research Center Institutional Animal Care and Use Committee standards and guidelines (IACUC #1392).

Zebrafish lines and maintenance

Zebrafish (*Danio rerio*) were staged and maintained according to standard procedures as previously described (Kimmel et al., 1995). All transgenic lines were maintained in the *AB background. Transgenic lines used in this study include *Tg(isl1CREST-hsp70l:mRFP)*^{fh1} (Grant and Moens, 2010), *Tg(ptf1a:egfp)*^{jh1} (Godinho et al., 2005), *Tg(UAS:kaede)*^{s1999} (Davison et al., 2007), gift of the Baier lab, *Tg(hsp70l:dnfgf1r-EGFP)*^{pd1} (Lee et al., 2005), *Tg(hsp70:TCFΔC-GFP)*^{w74} (Martin and Kimelman, 2012), gifts of the Kimelman lab, *Tg(atoh1a:EGFP)*^{nns7} (Kani et al., 2010) and *Tg(atoh1a:dTomato)*^{nns8} (Wada et al., 2010), gifts of the Hibi lab.

Fgf and Wnt signaling inhibition

Fgf and Wnt signaling was blocked by incubating 10 hpf embryos containing the heat-inducible *Tg(hsp70l:dnfgfr-EGFP)*^{pd1} or *Tg(hsp70:TCFΔC-GFP)*^{w74} for 15 minutes at 38°C or 40°C, respectively (Lee et al., 2005; Martin and Kimelman, 2012).

Notch signaling inhibition

Notch signaling was blocked by incubating 4 hpf embryos in a final concentration of 50 uM DAPT (Sigma D5942) diluted in embryo media for the amount of time as indicated in the figure

legend. Vehicle control embryos were incubated in embryo media containing a final concentration of 0.5% DMSO for the same amount of time as DAPT-treated embryos.

Retrograde labeling

5 dpf embryos were anesthetized with 0.4% ethyl 3-aminobenzoate methanesulfonate (ms-222), mounted in 1.2% agar, and a caudal transsection was made with a scalpel immediately after the yolk sac. Rhodamine-dextran (10,000 mw, Invitrogen) was applied to the incision. Animals were unmounted and allowed to rest for 3 hr and then fixed in 4% paraformaldehyde with 1x PBS (phosphate-buffered saline) and 4% sucrose at 4°C overnight and then processed for immunostaining (see "Immunofluorescence").

EdU labeling

Starting at 3 dpf, embryos were incubated in final concentration of 0.5 mM F-ara-EdU (Sigma T511293) diluted in fish water. Half of the solution was replaced on the second day of treatment. Embryos were anesthetized and fixed at 5 dpf. For EdU visualization, fixed whole embryos were permeablized in PBSTr (PBS + 0.5% Triton X-100) for 30 mins at RT and then incubated in a solution containing 10uM Cy5-azide (Lumiprobe A2020), 2 mM copper(II) sulfate (Sigma 45167), and 20 mM sodium ascorbate (Sigma A7631) for 1 hour at RT. After 3 PBS washes, samples were processed for immunostaining as described below ("immunofluorescence").

Generation of mutant alleles

atoh1a^{fh282} was generated by TILLING (Draper et al., 2004) and has been previous described (Pujol-Marti et al., 2012). *atoh1b*^{fh473} was generated with use of CRISPR/Cas9 as outlined in

(Shah et al., 2015). The CRISPR gRNA sequences for *atoh1b* were: 5'-GGCTGACCCGGAGTGACCCG and 5'-GGTGCGTGCGTAATTCTCCA. *atoh1c*^{fh367} was generated with the use of TALENs as outlined in (Sanjana et al., 2012). The TALEN target sequences for *atoh1c* were as follows: 5'-GGAGAGAGACTGACAGATC and 5'-CCAGCCCATTGGGGCTTT. In each experiment, embryos were phenotyped blind and then later genotyped by PCR using the following protocols: *atoh1a*^{fh282}: forward primer 5′-ATGGATGGAATGAGCACGGA and reverse primer 5′-GTCGTTGTCAAAGGCTGGGA followed by digestion with AvaI (New England Biolabs) generates a 195 bp + 180 bp WT allele and a 195 bp + 258 bp mutant allele; *atoh1b*^{fh473}: forward primer 5′-TGGACACTTTCGGGAGGAGT and reverse primer 5-CTTCAGAGGCAGCTTGAGGG generates a 180 bp WT allele and a 125 bp mutant allele; *atoh1c*^{fh367}: forward primer 5′-GACTCCCTGTGGTCATTATCAA and reverse primer 5′-AGCTCACTCAGGGTGCTGAT generates a 510 bp WT allele and a 388 bp mutant allele.

Plasmid construction and injection

TgBAC(atoh1c:gal4ff)^{fh430} was generated according to the protocol outlined in (Bussmann and Schulte-Merker, 2011) and using BAC recombineering plasmids provided by the Shulte-Merker lab. A BAC containing *atoh1c* (#38G3) was obtained from the BACPAC Resources Center at Children's Hospital Oakland Research Institute. This BAC was recombineered to insert *gal4ff* 114 bp downstream of the *atoh1c* ATG and to add *tol2* arms flanking the genomic DNA insert. *Tg(UAS:kaede)*^{s1999} embryos were injected at the one-cell stage with 180 pg of the modified BAC along with 90 pg of *tol2 transposase* mRNA. Expressing embryos were raised to adulthood for the establishment of stable transgenic lines.

RNA *in situ* hybridization

For all *in situ* hybridizations, embryos were fixed in 4% paraformaldehyde with 1x PBS (phosphate-buffered saline) and 4% sucrose at 4°C overnight. RNA *in situ* hybridization was performed as described (Thisse et al., 1993). Embryos were mounted in glycerol on coverslips and transmitted light images were taken on a Zeiss Axioplan2 microscope.

Live imaging

Embryos were anesthetized with 0.4% ethyl 3-aminobenzoate methanesulfonate (ms-222) (Sigma) and immobilized in 1.2% low-melting point agarose (Gibco). All embryos were imaged on a Zeiss LSM700 inverted confocal microscope.

Immunofluorescence

For immunostaining, embryos were fixed in 4% paraformaldehyde with 1x PBS and 4% sucrose at 4°C overnight. The fixed embryos were washed with PBSTr (PBS + 0.5% Triton X-100), dissected and incubated in acetone at −20 °C for 7 min. Dissected brains were washed once with PBSTr and twice with PDT (PBS, 1% BSA, 1% DMSO, 0.5% Triton X-100), and incubated in 5% goat serum in PDT at RT for 2 h. The samples were incubated with the primary antibody solution at 4 °C overnight. After four washes with PBST, the tissues were incubated with secondary antibodies (1/500 dilution, Alexa Fluor 488 and/or Alexa Fluor 594 goat anti-mouse and/or goat anti-rabbit IgG (H + L), (Molecular Probes, Invitrogen). Following staining, tissue was cleared step-wise in a glycerol series and mounted for confocal imaging. The following antibodies were used: chicken anti-GFP (1:500, Abcam); rabbit anti-Kaede (1:500, MBL Co.

Ltd.); mouse anti-HuC/D (1:500, Invitrogen); mouse anti-TH (1:500, Millipore); mouse anti-CHaT (millipore,1:500); anti-RFP (1:1000, Abcam); mouse anti-NeuroD1(1:500, gift from the Hibi Lab).

Chimeric analysis

atoh1c^{fh367}*, dnFgfr,* or *TCFΔC* embryos or wildtype controls to be used as donors in transplantation experiments were injected at the 1-cell stage with either Cascade Blue-dextran or Rhodamine-dextran (10,000 mw, Invitrogen). Cells were transplanted from these donor embryos into wild-type or *atoh1c*^{fh367} mutant host embryos at the early gastrula stage as described (Kemp et al., 2009), targeting donor cells to the dorsal CNS at the mid-hindbrain level of host recipients. Donor embryos were raised to 3 dpf to determine which transgene(s) they carried, and/or were genotyped for the presence of the *atoh1c*^{fh367} allele. Hosts of donors of the relevant genotype(s) were imaged as described above ("Live Imaging").

Chapter 3: *atoh1* gene expression in the zebrafish hindbrain and characterization of early *atoh1c*-derivatives

Zebrafish *atoh1* genes are expressed sequentially at the URL

To determine the expression dynamics of the *atoh1* genes during cerebellar development, we carried out a time-series RNA *in situ* hybridization analysis. Consistent with previous reports, we found that all three *atoh1* homologues are expressed in the URL beginning from 1 day post fertilization (dpf) and persists beyond 5 dpf, as previously described (Fig. 2) (Chaplin et al., 2010; Kani et al., 2010). In addition, we identified a previously undescribed *atoh1c* expression domain at the mid-hindbrain boundary (MHB), anterior to the presumptive URL. This expression domain is detected by RNA *in situ* hybridization starting at 14 hpf until 30 hpf (Fig. 2A,B) at which point it is extinguished and expression in the URL comes on from 2 dpf until our analysis end point, 5 dpf (Fig. 2G,H,M,N). Both *atoh1a* and *atoh1b* are expressed in the URL beginning at 24 hpf (not shown), but by 5 dpf their expression is largely restricted to the Va, a progenitor zone in the anterior-most region of the cerebellum (Fig. 2C-F, I-L) (Kani et al., 2010; Kaslin et al., 2009). Although *atoh1b* is primarily expressed in the Va region at 5 dpf, weak expression is also detected in the URL and at the midline of CCe (Fig. 2K,L, light blue and gray arrowheads) where *atoh1c* is strongly expressed (Fig. 2M,N).

Regulation of early *atoh1c* expression domain

The early expression domain of *atoh1c* lies at the MHB, an important signaling center required for early development of both the midbrain and hindbrain (Rhinn and Brand, 2001). Double RNA *in situ* hybridization with *otx2* and *gbx2*, which are expressed anterior and posterior

to the MHB, respectively, demonstrated that *atoh1c* is expressed in a few cells immediately posterior to the boundary (Fig. 3A,B). The position of the MHB is determined by the interface of Otx2 and Gbx2 and is reciprocally maintained by Wnt1 expression anterior to the boundary and Fgf8 expression posterior to the boundary. Not surprisingly, MHB *atoh1c* expression is lost under conditions where Fgf and Wnt signaling are blocked by heat-inducible expression of dominant negative (dn) FGFR1 or dnTCFΔC, respectively (Fig. 3E-G) (Lee et al., 2005; Martin and Kimelman, 2012). To investigate the nature of this requirement, we made chimeras in which cells expressing dnFGFR1 or dnTCFΔC and a transgenic *atoh1c* reporter (see below) contributed sparsely to the MHB region. In these chimeras, dn expressing cells are cell-autonomously blocked for Fgf or Wnt signaling, but the MHB morphogenetic program occurs normally in the surrounding wildtype cells. Whereas non-dn-expressing cells at the MHB expressed the *atoh1c* reporter (n=10/10 chimeric embryos; Fig. 3H), cells expressing dnFGFR1 or TCFΔC at the MHB never expressed the *atoh1c* reporter (n=0/32 chimeric embryos; Fig. 3I,J). Thus the tightly restricted expression of *atoh1c* to progenitors at the MHB is because cells must be able to perceive both Wnt and Fgf signals in order to express *atoh1c.*

In addition to regulation by Wnt and Fgf signaling pathways, we have found that the early *atoh1c* expression domain is subject to Notch-mediated lateral inhibition. This well-studied process starts when a proneural gene non-autonomously limits its own expression by transcriptional activation of Delta, which in turn stimulates Notch in adjacent cells to inhibit proneural gene expression there. This process is amplified through a field a cells until a single progenitor expresses high levels of the proneural gene and acquires the “primary” cell fate – in the nervous system this is the neuronal fate (Artavanis-Tsakonas et al., 1999). When we pharmacologically inhibit Notch signaling with γ-secretase inhibitor DAPT (Geling et al., 2002)

we find that the *atoh1c* expression domain is expanded to double the number of expressing cells (~20 cells) compared to vehicle-treated controls at 22 hpf (Fig. 4A). The expansion of the *atoh1c* expression domain in DAPT-treated embryos results in the generation of ectopic neurons (see below about identity of neuronal population) which we can visualize using an *atoh1c* transgenic reporter (see below about transgenic reporter; Fig. 4A,B). In addition, we also see double the number of *atoh1c*-expressing cells at 22 hpf in *atoh1c* mutants by RNA *in situ* hybridization (data not shown), another phenotype consistent with the classic lateral inhibition model. Atoh1c expression is still restricted to the MHB because of its requirement for MHB-derived Wnt and Fgf signaling. Our results provide additional evidence of active Notch signaling at the MHB early in development and a proneural function for Atoh1c at the MHB.

***atoh1c* isthmic domain gives rise to ventral r1 neurons related to the Locus Coeruleus**

In order to visualize the *atoh1c*-derived cell populations *in vivo*, we generated an *atoh1c* transgenic reporter, *TgBAC(atoh1c:gal4ff)fh430,* by BAC recombineering combined with *tol2 transposase*-mediated transgenesis (Fig. 5A-L) (Bussmann and Schulte-Merker, 2011). When crossed to *Tg(UAS:kaede)s1999t* (Scott et al., 2007), our *TgBAC(atoh1c:gal4ff)fh430* driver (hereafter referred to as *Tg(atoh1c::kaede)* for simplicity) recapitulates all aspects of endogenous *atoh1c* expression at the MHB and URL. Taking advantage of the long-lived nature of the photoconvertible Kaede fluorescent protein (Ando et al., 2002; Caron et al., 2008) we were able to follow the fate of the MHB *atoh1c*+ progenitor pool after *atoh1c* mRNA expression at the MHB was extinguished. Starting at 20 hpf, the MHB *Tg(atoh1c::kaede)*+ population migrates ventrocaudally to rhombomere 1 (r1) ventral to the presumptive cerebellum and gives rise to bilateral comma-shaped nuclei consisting of about 20 neurons by 2 dpf (Fig. 5A-F, O). Since the

onset of *atoh1c* expression at the URL at 3 dpf complicates the subsequent lineage analysis of MHB-derived *atoh1c* neurons (see below for further discussion of *atoh1c* URL derivatives), we distinguished the MHB-derived *atoh1c* lineage by photoconverting the Kaede+ MHB domain at 22 hpf, before the onset of URL expression (Fig. 5M-P). We found that the majority of neurons present in ventral r1 are Kaede Red+ indicating they originated from the *atoh1c*+ MHB progenitor domain.

In an effort to identify the *Tg(atoh1c::kaede)*+ neurons, we began with a literature search to compile a list of all known zebrafish neuronal populations located in close proximity to the ventral rhombomere 1 neurons in question. Using that approach we determined that the following populations may be in a close or overlapping region: Ptf1a+ Purkinje neurons, Islet1+ oculomotor neurons (CNIII and CNIV), the nucleus of the medial longitudinal fasciculus (nucMLF) and Locus Coeruleus (LC). Using both transgenic reporters and retrograde labeling we found that the *Tg(atoh1c::kaede)*+ population does not overlap with Purkinje and oculomotor neurons as well as the nucMLF (Fig. 6A-C, gray arrowheads). However, from the retrograding labeling we determined that a small subset (~4 cells) of the *Tg(atoh1c::kaede*)+ neurons are likely reticulospinal neurons located in r1 (Fig. 6C, yellow cells). In addition, we used immunostaining and RNA *in situ* hybridization to determine whether the *Tg(atoh1c::kaede)*+ neurons were positive for GABAergic (*glutamate decarboxylase 1b*; Fig. 6D), cholinergic (Choline Acetyltransferase; Fig. 6E), or nitric oxide (*nitric oxide synthase 1*; Fig. 6D) markers. We find that there is no overlapping expression between those markers and *atoh1c::kaede* transgene. Next, we sought to determine if the *Tg(atoh1c::kaede)*+ r1 neurons overlapped with the Locus Coeruleus.

The migratory path from the MHB of these *atoh1c*+ neurons and their final position in r1 are reminiscent of the Locus Coeruleus (Chiu and Prober, 2013; Guo et al., 1999). The LC is a noradrenergic neuronal population present in all vertebrates that controls arousal. At 5 dpf, the *Tg(atoh1c::kaede)*+ neurons lie immediately anterior to the LC and have overlapping contralateral and longitudinal projections with them (Fig. 5R-T) (Guo et al., 1999). Furthermore, the *Tg(atoh1c::kaede)*+ r1 neurons express the biosynthetic enzyme tyrosine hydroxylase (TH) during their migration (Fig. 5R,S, gray arrowheads), however, the *atoh1c*+ r1 neurons are not the LC neurons themselves as they eventually turn off TH while the neurons of the LC maintain it (Fig. 5T). Given the similarities between these two populations, we hypothesize that the *Tg(atoh1c::kaede)*+ r1 neurons may be functionally connected to the LC and a part of the arousal circuit as well.

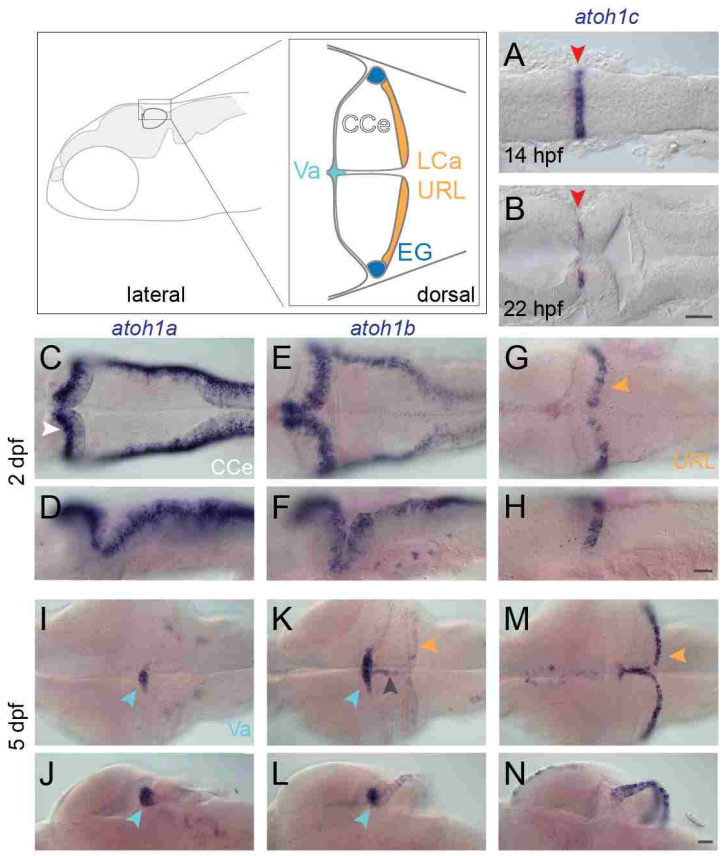

Figure 2. *atoh1* gene expression in the developing zebrafish cerebellum.

Schematic depicts regions of the zebrafish cerebellum in lateral (left panel) and dorsal (right panel) views. Throughout the document, white arrowheads indicate the CCe, light blue arrowheads indicate the Va, orange arrowhead indicate the URL (at early stages) or the LCa (at later stages) and dark blue arrowheads indicate the EG. Red arrowheads indicate the position of the MHB. A-N: RNA *in situ hybridization* in wild-type embryos with *atoh1a* (left column), *atoh1b* (middle column), and *atoh1c* (right column) at 14 hpf (A) 22 hpf (B), 2 dpf (C-H), and 5 dpf (I-N). Dorsal (A,B,C,E,G,I,K,M) or lateral (D,F,H,J,L,N) views are shown with anterior to the left. Gray arrowhead in this figure indicates midline of CCe. CCe, corpus cerebelli; EG, eminentia granularis; LCa, lobus caudalis cerebelli; URL, upper rhombic lip; Va, valvula cerebelli; Scale bars: 50 uM.

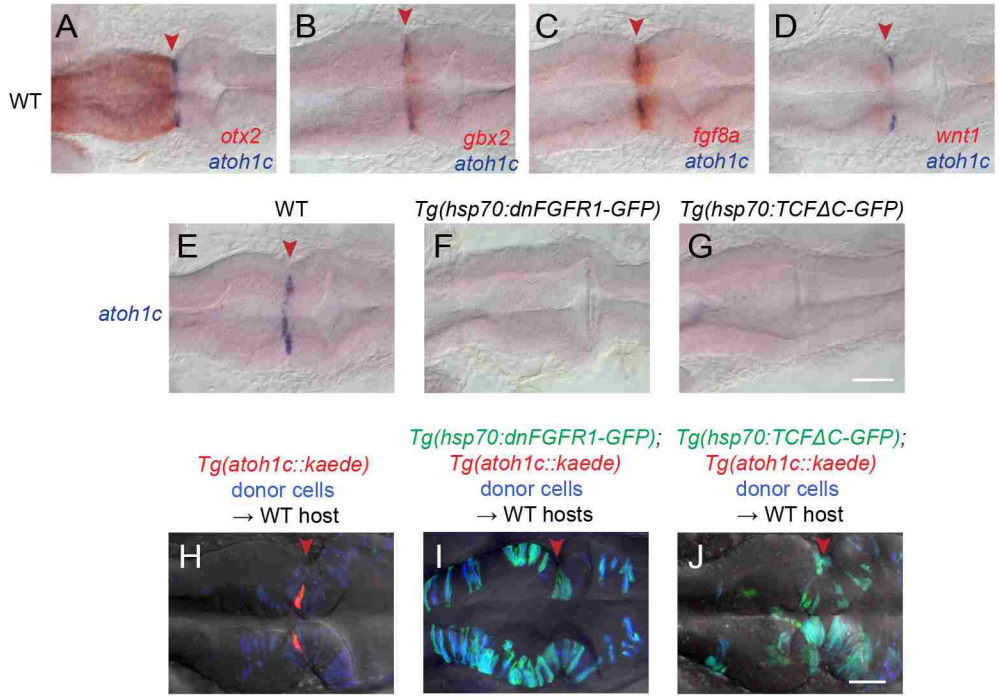

Figure 3. Specification of the *atoh1c* MHB domain.

A-D: Double RNA *in situs* for *atoh1c* (blue) and *otx2* (A), *gbx2* (B), *fgf8* (C), and *wnt1* (D) (red) show that the *atoh1c* expression domain is in a few cells immediately posterior to the MHB. E-G: *atoh1c* expression is absent when Fgf (F) or Wnt (G) signaling is blocked with heat-inducible dominant-negative transgenes activated at 10 hpf. H-J: *atoh1c* expression requires cell-autonomous Fgf and Wnt signaling. Live imaging of chimeras with donor-derived cells (blue) expressing dn-FGFR1 (I, green) or dn-TCFΔC (J, green) that are unable to express *Tg(atoh1c::kaede)* (red in the control chimera in H) even if they lie at the MHB (red arrowheads). All embryos are at 22 hpf and are shown in dorsal views with anterior to left. Scale bars: 50 µM. Experiments in this figure were performed by Chen-Ying Su.

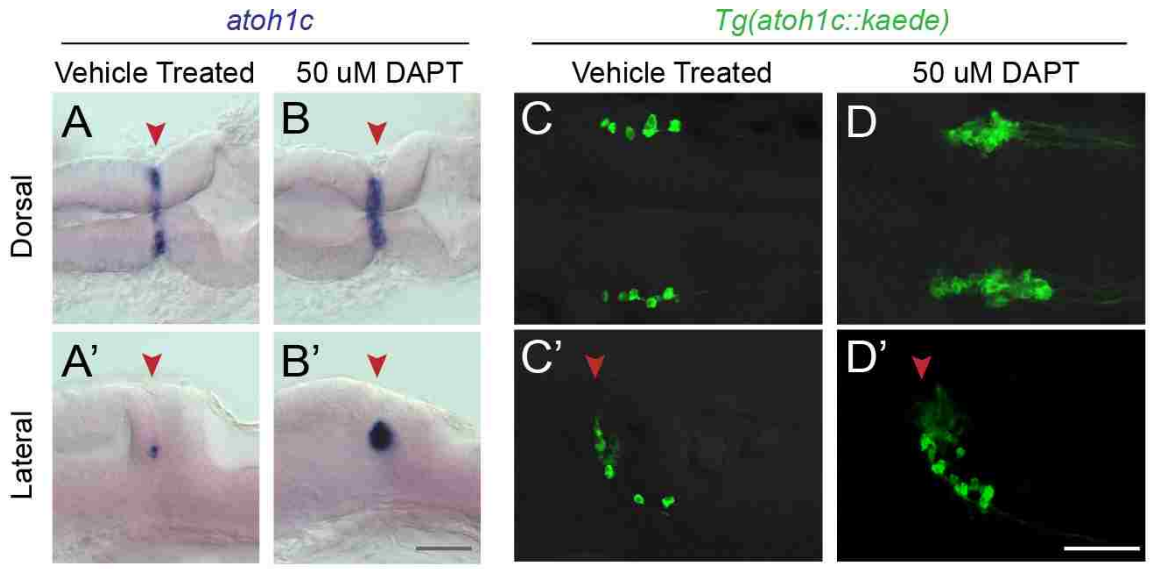

Figure 4. Notch-mediated lateral inhibition of *atoh1c* MHB domain.

Pharmacological inhibition of Notch signaling with γ-secretase inhibitor DAPT blocks restriction of *atoh1c* expression domain (B) resulting in an overproduction of *Tg(atoh1c::kaede)*+ neurons (D) compared to stage-matched vehicle treated control embryos (A, C). 22 hpf embryos (A,B) treated for 18 hours or 30 hpf embryos (C,D) treated for 26 hours in orientations as indicated. Red arrowheads indicate location of MHB. Scale bars: 50 uM.

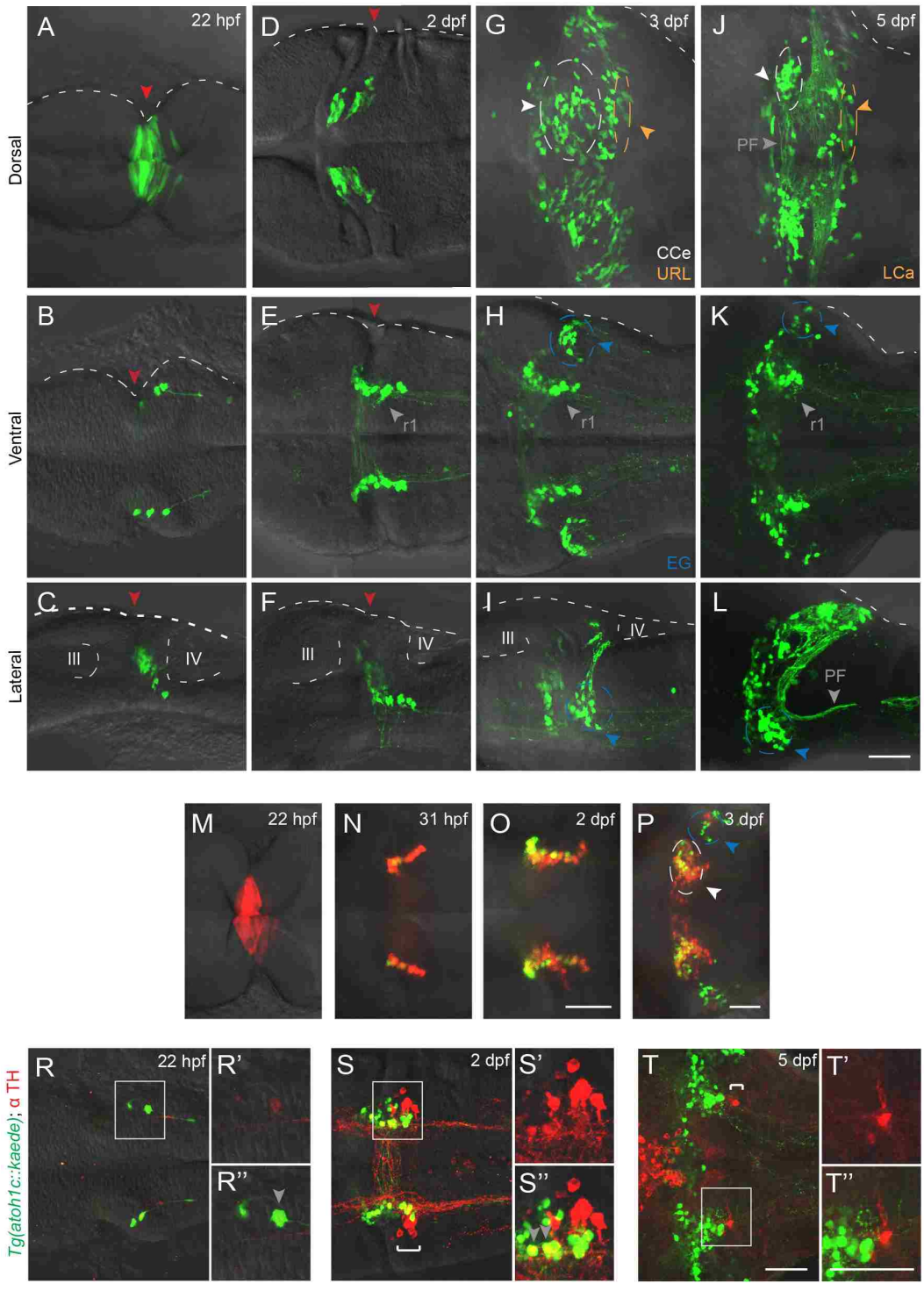

Figure 5. *atoh1c*-expressing progenitors give rise to to ventral r1 and cerebellar granule neurons.

A-L: *Tg(atoh1c::kaede)* transgene expression in fixed embryos stained with anti-Kaede antibody in dorsal (A,D,G,J), ventral (B,E,H,K) and lateral (C,F,I,L) views at 22 hpf (A-C), 2 dpf (D-F), 2 dpf (G-I) and 5 dpf (J-L). Arrowheads follow the color code described in Fig. 2 legend or are labeled as follows: PF: parallel fibers, r1: MHB-derived neurons in ventral r1. M-P: live imaging after photoconversion of Kaede of MHB *atoh1c*+ cells at 22 hpf confirms that this Tg(*atoh1c::kaede)*+ progenitor domain gives rise to ventral r1 neurons. Dorsal (M) and ventral focal planes (N-P). R-T: *Tg(atoh1c::kaede)*+ cells (green) transiently express TH (red; gray arrowheads) from 22 hpf to 2 dpf and lie adjacent to the LC (indicated by white bracket). All images oriented with anterior to the left at time points as indicated. Scale bars: 50 μM.

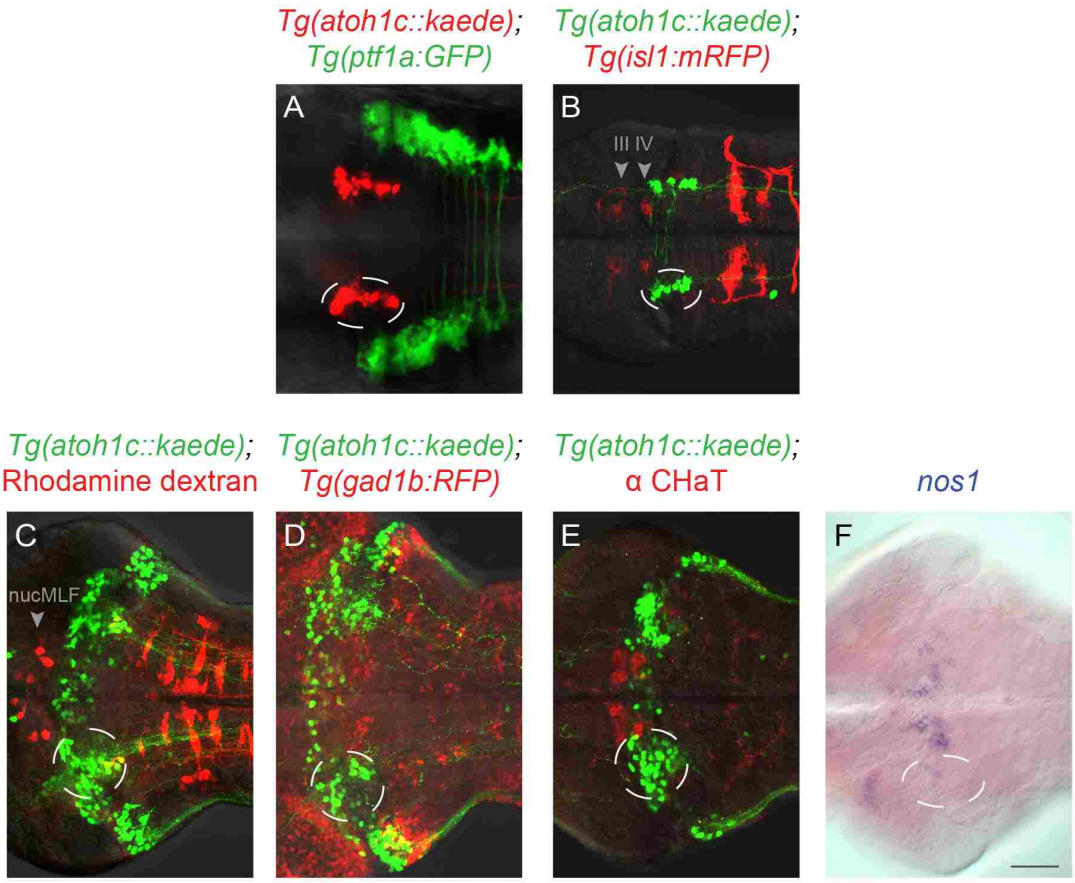

Figure 6. Position of ventral rhombomere 1 neurons in relation to known neuronal populations.

Use of transgenes (A,B,D), retrograde labeling (C), immunostaining (E), and RNA *in situ* hybridization (F) to determine if there is overlap between *Tg(atoh1c::kaede)*+ ventral r1 neurons and neighboring populations. Combining *Tg(atoh1c::kaede)* with other transgenic reporters indicate its location relative to *ptf1a*+ Purkinje neurons (A) and *islet1*+ oculomotor motor nuclei (B; gray arrowheads). Retrograde labeling with rhodamine dextran indicates a small subset of *Tg(atoh1c::kaede)*+ neurons are reticulospinal neurons (yellow) and do not overlap with the nucleus of the medial longitudinal fasciculus (C, gray arrowhead indicates nucMLF). *Tg(atoh1c::kaede)* cells do not express nitric oxide synthase 1 (F; *nos1*). Ventral focal planes with anterior to the left. A, B: 2 dpf, C-F: 5 dpf. Scale bar: 50 μM.

Chapter 4: Role of *atoh1* genes in the development of cerebellar neurons

Atoh1c is required for the specification of granule neurons in the zebrafish cerebellum

By 3 dpf, the majority of the *Tg(atoh1c::kaede)*+ cells in the cerebellum have migrated to regions populated by granule neurons: the CCe, EG and LCa (Fig. 5G-L, Movie 1). Their axons appear starting at 3.5 dpf and resemble granule neuron parallel fibers (Hibi and Shimizu, 2012; Takeuchi et al., 2015b). Given the location and projections of the *Tg(atoh1c::kaede)*+ population we conclude that they are granule neurons of the CCe, EG, and LCa. *Tg(atoh1c::kaede)*+ granule neurons are not detected in the Va, where many of the *atoh1a*-derived granule neurons are located (Kani et al., 2010).

To directly assess the function of Atoh1c in granule neuron development, we used with transcription activator-like effector nucleases (TALENs) to generate a 122 bp deletion (fh367) that results in a premature stop before the DNA binding domain. Expression of *cerebellin12* (*cbln12*), a marker of all mature granule neurons (Takeuchi et al., 2016), is strongly reduced in the CCe, EG and LCa in *atoh1c*^{fh367} mutants (Fig. 7A,B). A marker of glutamatergic cerebellar granule neurons, *vesicular glutamate transporter 1 (vglut1),* is similarly reduced at both the mRNA (Fig. 7C,D) and protein levels (not shown). Majority of the *Tg(atoh1c::kaede)*+ cells accumulate at the URL in *atoh1c*^{fh367} mutants, where they strongly express *atoh1c* mRNA (Fig. 7G compare to Fig. 2M,N), retain a neural progenitor-like morphology, and elaborate comparatively few parallel fibers (Fig. 7E,F compared to Fig. 5G,I,J,L; Movie 2). Thus *atoh1c* contributes to the specification of granule neurons located in the CCe, LCa, and EG.

If *atoh1c* is required for the development of granule neurons, then we predict one or more aspects of granule neuron maturation are defective in the mutant. Using markers of post-mitotic

neurons (HuC/D; (Kim et al., 1996)), committed granule neuron precursors (NeuroD1; (Kani et al., 2010)) and cell proliferation (EdU incorporation) we determined the differentiation state of the *atoh1c*^{fh367} cells (Fig. 8). It is important to note that due to epigenetic silencing of the UAS element (Akitake et al., 2011), not all of the *atoh1c*-derived granule neurons are detectable in a given fish using the *atoh1c::kaede* transgene. In 5 dpf wild-type larvae, the majority of *Tg(atoh1c::kaede)*+ cells have migrated away from their birthplace at the URL although a small population of HuC/D+ (Fig. 8A), NeuroD1+ (Fig. 8C) granule neurons remain near the URL in the LCa where, together with granule neurons in the EG, they contribute to the parallel fibers that project to the cerebellar-like structure in the hindbrain (Takeuchi et al., 2015b). In contrast, in the *atoh1c* mutant, the majority of the *Tg(atoh1c::kaede)*+ cells remain at the URL but do not express HuC/D or elaborate axons (Fig. 8B), but they do express NeuroD1 (Fig. 8D) suggesting that they are committed but undifferentiated granule neuron precursors. To determine whether these are proliferating progenitors, we exposed 3 dpf larvae to 5-ethynyl-2'-deoxyuridine (EdU) continually for two days before fixing at 5 dpf (Fig. 8E,F). Any cells that were proliferating during that period will incorporate EdU. In the *atoh1c* mutant, the massively expanded *Tg(atoh1c::kaede)*+ population in the URL is post-mitotic during this period (Fig. 8F). This post-mitotic but undifferentiated progenitor state with strongly increased *atoh1c* mRNA expression in *atoh1c* mutants (Fig. 7G) is consistent with a classic proneural function for Atoh1c in the URL as has previously been proposed (Gazit et al., 2004; Machold et al., 2007; Millimaki et al., 2007).

Atoh1c cell-autonomously promotes delamination from URL

Loss of *atoh1c* results in the accumulation *atoh1c*-expressing granule neuron precursors in the URL that are unable to terminally differentiate. How does a differentiation-arrested committed precursor behave? In order to address this, we performed high-resolution time-lapse imaging of both wildtype and *atoh1c*^{fh367} embryos at 3 dpf, a time when we can continuously capture the birth and migration of granule neurons. Before migrating, wildtype *atoh1c*-expressing progenitors are epithelial, with their apical end feet along the ventricle-facing surface of URL (Fig. 9A-D, Movie 3). They elaborate a basal process and very soon thereafter they release their apical contact and move away from the URL following this basal process (Koster and Fraser, 2001; Volkmann et al., 2010). This transition is accomplished in a period of six hours (Fig. 9A-D, Movie 3). In contrast, *atoh1c* mutant progenitors at the URL elaborate highly dynamic basal processes but fail to detach from the epithelium during the same period (Fig. 9E-H, Movie 4). Interestingly, "escaper" neurons in *atoh1c* mutants complete granule neuron differentiation and elaborate parallel fibers (Fig. 7F, cells in CCe). To determine if detachment from the URL is a cell-autonomous function of *atoh1c* we generated genetic chimeras. In chimeras, *atoh1c* mutant cells migrated equally poorly from the URL when surrounded by WT cells (48% cells migrated; n=422 cells, 10 embryos) as when surrounded by *atoh1c* mutant cells (56% cells migrated; n=122 cells, 21 embryos). Conversely, wildtype cells migrated equally well when surrounded by mutant cells (72% cells migrated; n=284 cells, 11 embryos) as by wildtype cells (77% cells migrated; n=53 cells, 15 embryos). Thus, Atoh1c promotes the release of the granule neuron precursors from the URL epithelium, an essential step in neuronal differentiation (Hartenstein et al., 1992; Pacary et al., 2012).

Atoh1 paralogs function redundantly in granule neuron differentiation

Given their overlapping expression in the URL (Fig. 2), we were interested in understanding the functional relationships between the *atoh1* homologues. We generated mutant alleles for *atoh1a* and *1b*. The *atoh1a*^{fh282} allele is a missense mutation upstream of the predicted DNA binding domain and has been shown to have a loss-of-function phenotype in the zebrafish lateral line (Pujol-Marti et al., 2012). The *atoh1b*^{fh473} allele is a 55 bp deletion that truncates the protein upstream of the predicted DNA binding domain. *atoh1a* and *atoh1c* are expressed independently of each other whereas the expression of *atoh1b* is regulated by *atoh1c* in regions of overlapping expression: the URL and midline of the CCe (not shown). Loss of *atoh1a* and *atoh1b* alone have no detectable effects on *cbln12* expression and the migration and differentiation of *Tg(atoh1c::kaede)*+ cells (Fig. 10B,C). In addition to its expression in the URL, *atoh1a* is also expressed throughout the hindbrain lower rhombic lip (LRL) which gives rise to a range of commissural interneurons and pre-cerebellar nuclei in mice (Bermingham et al., 2001; Helms and Johnson, 1998; Rose et al., 2009a). Using an *atoh1a* reporter (*Tg(atoh1a:EGFP)nns7)* (Kani et al., 2010), we found that many *Tg(atoh1a:EGFP)*+ cells are retained at the LRL with a neural progenitor-like morphology in *atoh1a*^{fh282} mutants suggesting a role for *atoh1a* in commissural interneuron differentiation as has been described in the mouse (Fig 11B).

Although we observe a large reduction of mature granule neurons in the *atoh1c* mutant, some residual *cbln12* and *vglut1* expression remains, particularly in the CCe (Fig. 7B,D). To test possible redundancy amongst *atoh1* genes in granule neuron differentiation, we generated all possible *atoh1*$^{-/-}$ allelic combinations. We found that in *atoh1a*^{fh282}*; atoh1c*^{fh367} double mutant

there was a near-complete loss of *cbln12* expression (Fig. 10E'). This was not further enhanced in the *atoh1a*^{fh282}*; atoh1c*^{fh367}; *atoh1b*^{fh473} triple mutant (Fig. 10H') suggesting that *atoh1b* does not contribute detectably to granule neuron development. We conclude that *atoh1a* has a minor role in granule neuron differentiation in the CCe that is only detectable in the absence of *atoh1c.* This is consistent with previous lineage analysis that showed that only a minority of granule neurons in the CCe are derived from *atoh1a* progenitors (Kani et al., 2010).

atoh1a and *atoh1c* have distinct derivatives in the developing cerebellum

The enhanced granule neuron phenotype in *atoh1a*^{fh282}; *atoh1c*^{fh367} double mutants could be because either *atoh1a* expression partially compensates for loss of *atoh1c* in the same progenitor cells, or because *atoh1a* and *atoh1c* are independently required for the differentiation of two separate populations of granule neurons in the CCe, both of which express the pan-granule neuron marker *cbln12*. Consistent with the latter model, we detected no overlap in *Tg(atoh1c::kaede)* and *Tg(atoh1a:dtomato)*-expressing cells in double transgenic fish (Fig. 12) and in expression by double RNA *in situ* hybridization (not shown). We conclude that the *Tg(atoh1a:EGFP)*+ granule neurons within the CCe described by Kani et al. (Kani et al., 2010) represent a population of *cbln12*+ granule neurons distinct from the majority *Tg(atoh1c::kaede)*+ population. It remains to be seen whether these granule neuron populations do indeed play functionally distinct roles within the cerebellum.

atoh1a functionally rescues the *atoh1c*^{fh367} phenotype

A classic model for the maintenance of duplicated genes posits that regulatory changes render both genes essential for a subset of their pre-duplicated functions (Force et al., 1999). If

this is the case for *atoh1a* and *atoh1c*, we predict that either *atoh1a* or *atoh1c* could rescue granule neuron differentiation when expressed in the *atoh1c* progenitor domain in an *atoh1c*^{fh367} mutant. We sought to rescue the *atoh1c*^{fh367} phenotype by injection of a DNA construct encoding the full-length *atoh1a* cDNA under *atoh1c* regulation. We injected homozygous *atoh1c* mutant embryos carrying the *atoh1c:gal4ff* transgene at the one-cell stage with an *UAS:atoh1a-t2a-NLSmCherry* construct or a positive (*UAS:atoh1c-t2a-NLSmCherry*) or negative (*UAS:NLSmApple*) control construct, and determined the position of RFP-expressing cells at 4 dpf, using migration away from the URL as a proxy for the granule neuron differentiation. In these experiments, we used a very strict definition of "unmigrated" due to the nuclear localization of the RFP, scoring any cells with labeled nuclei that were not at the ventricular surface of the URL as "migrated". We thus likely underestimated the proportion of unmigrated neurons. Nevertheless, we found that *atoh1a* (95% cells migrated; n=42 cells, 19 embryos) and *atoh1c* (96% cells migrated; n=27 cells, 11 embryos) were equally effective in rescuing the migration of *atoh1c* mutant granule neurons, compared to *UAS:NLSmApple* alone (80% cells migrated; n=172 cells, 17 embryos) We conclude that *atoh1a* and *atoh1c* have equivalent functions in granule neuron progenitors, at least with respect to inducing delamination from the URL.

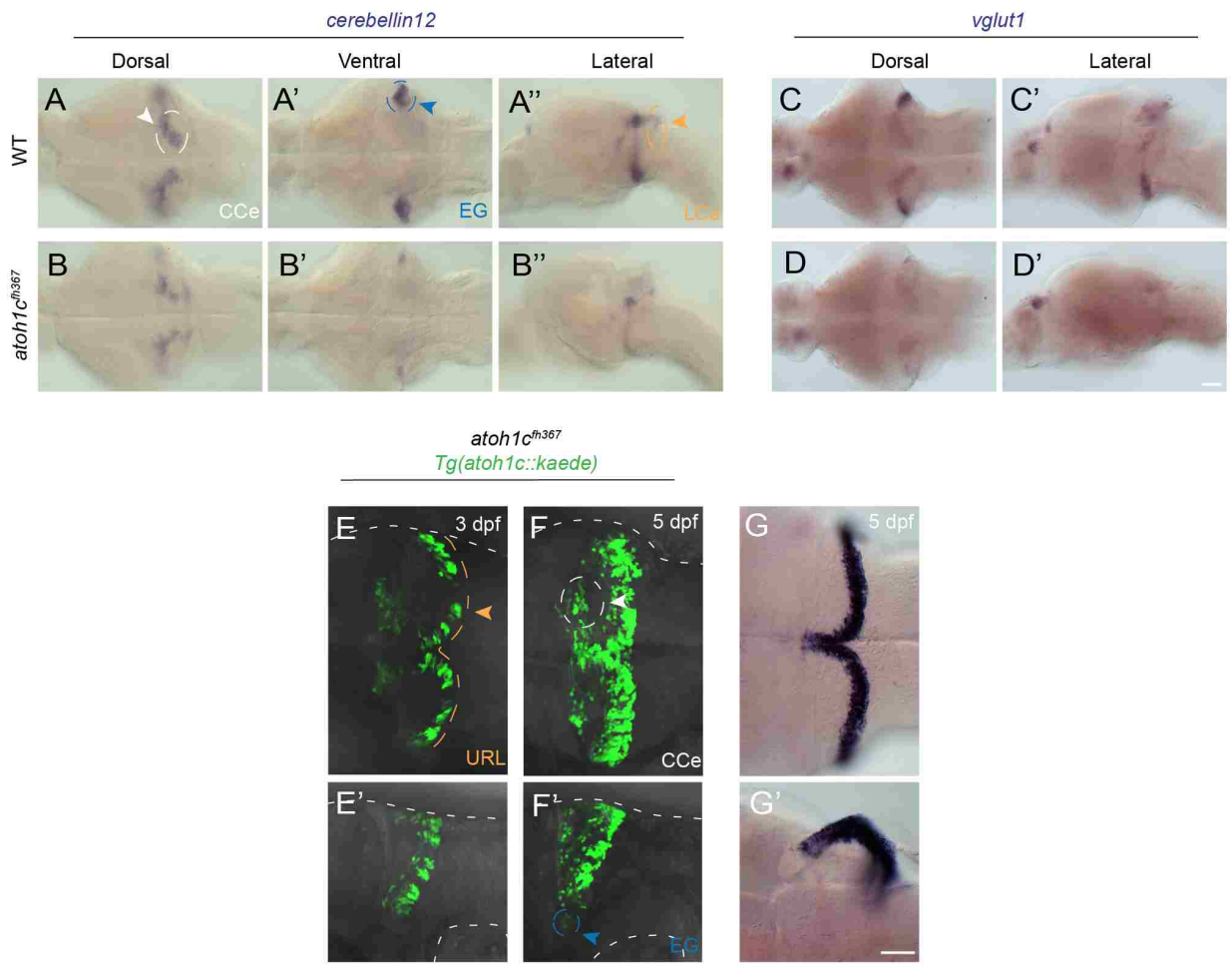

Figure 7. *atoh1c* is required for cerebellar granule neuron fate.

A-D: Reduction in the number of mature granule neurons in *atoh1c* mutant as indicated by decreased staining for *cerebellin12* (B) and *vglut1* (D), at 5 dpf. E-G: The majority of mutant cells expressing the *Tg(atoh1c::kaede)* remain as a non-migrated population in the URL at 3 dpf (E compare to wildtype in Fig. 5G,I) and 5 dpf (F compare to wild-type in Fig. 5J,L). G: Upregulation of *atoh1c* mRNA in URL at 5 dpf in *atoh1c* mutant embryos (compare to Fig. 2M,N). Dorsal (A-G) ventral (A', B') and lateral (A",B",C'-G') views are shown with anterior to the left. Scale bars: 50 μM.

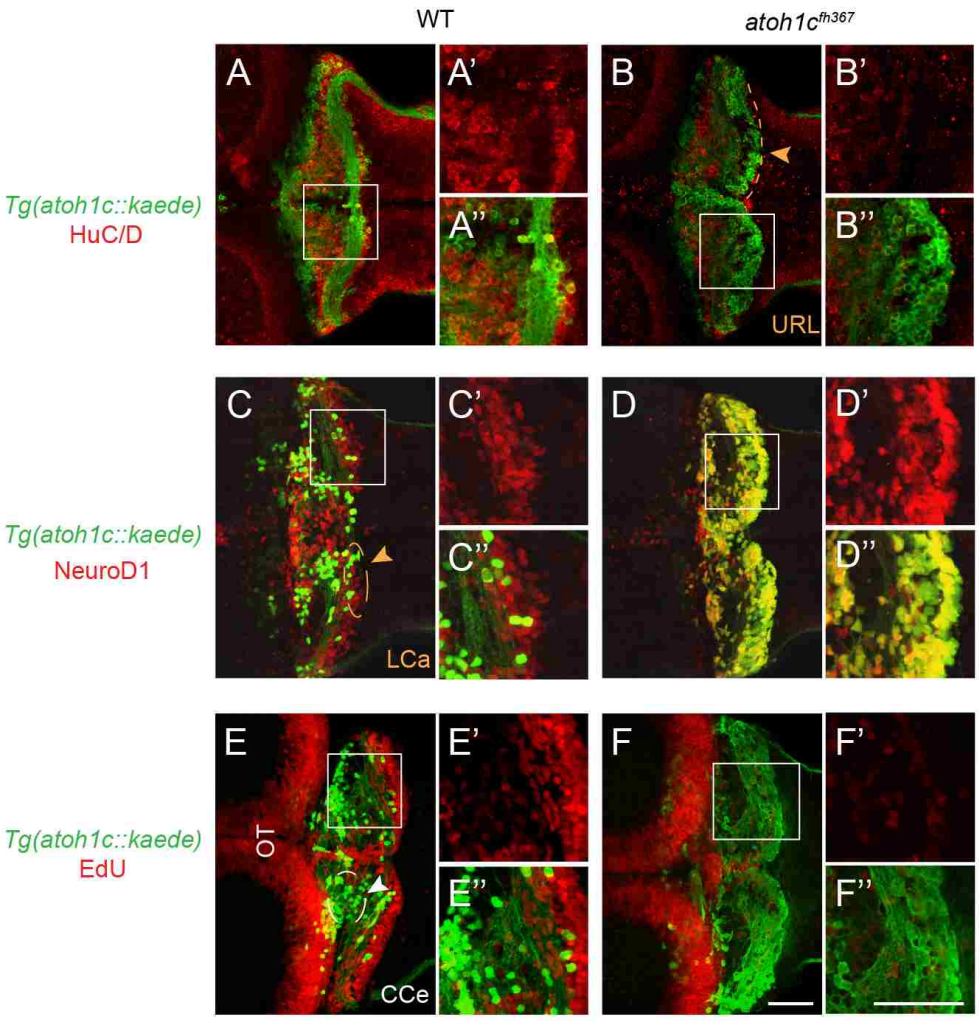

Figure 8. *atoh1c*^{fh367} cerebellar cells accumulate as post-mitotic but undifferentiated granule progenitors.

A,B: The majority of *Tg(atoh1c::kaede)*+ cells (green) in the *atoh1c* mutant are located within the URL and do not express HuC/D (red) at 5 dpf (B) indicating that they are not post-mitotic neurons. C,D: *atoh1c*^{fh367} cells (green) in the URL are positive for NeuroD1 (red). E,F: *atoh1c*^{fh367} cells (green) in the URL do not incorporate EdU (red). Strong EdU incorporation anterior to the cerebellum in both WT and mutant is in the optic tectum (OT). Dorsal views with anterior to the left. Scale bars: 50 μM.

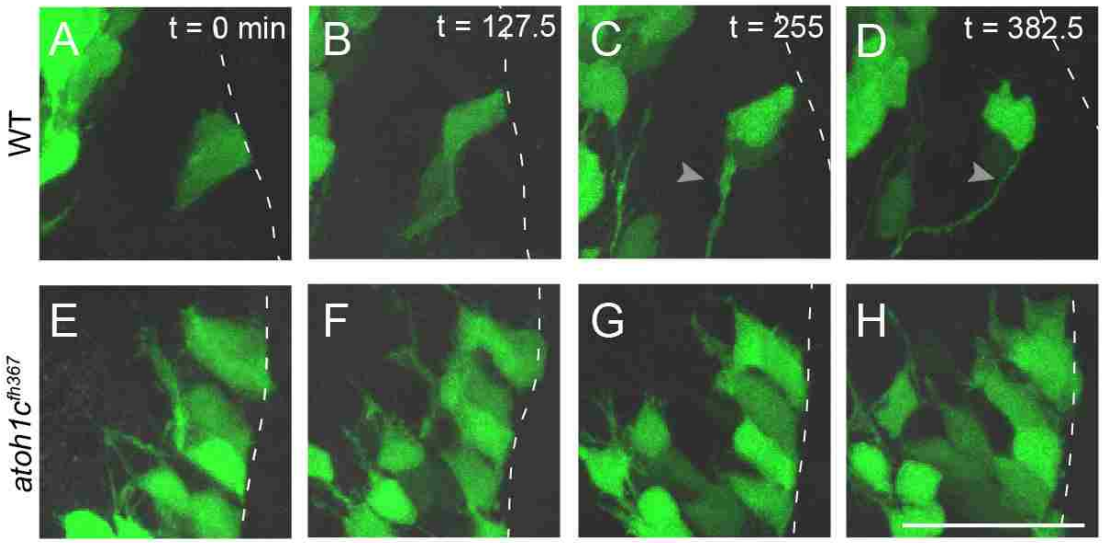

Figure 9. Atoh1c is required for release of granule neuron progenitors from URL.

Still images from confocal time-lapses taken at 3 dpf. Dotted line indicates the URL where the apical surfaces of granule neuron progenitors attach. In WT, *Tg(atoh1c::kaede)+* progenitors detach from the URL over a six-hour interval (A-D) while in *atoh1c* mutants *Tg(atoh1c::kaede)+* cells remain attached at the URL (E-H). Time (t) points indicated in upper right corner in minutes. Scale bar: 25 μM.

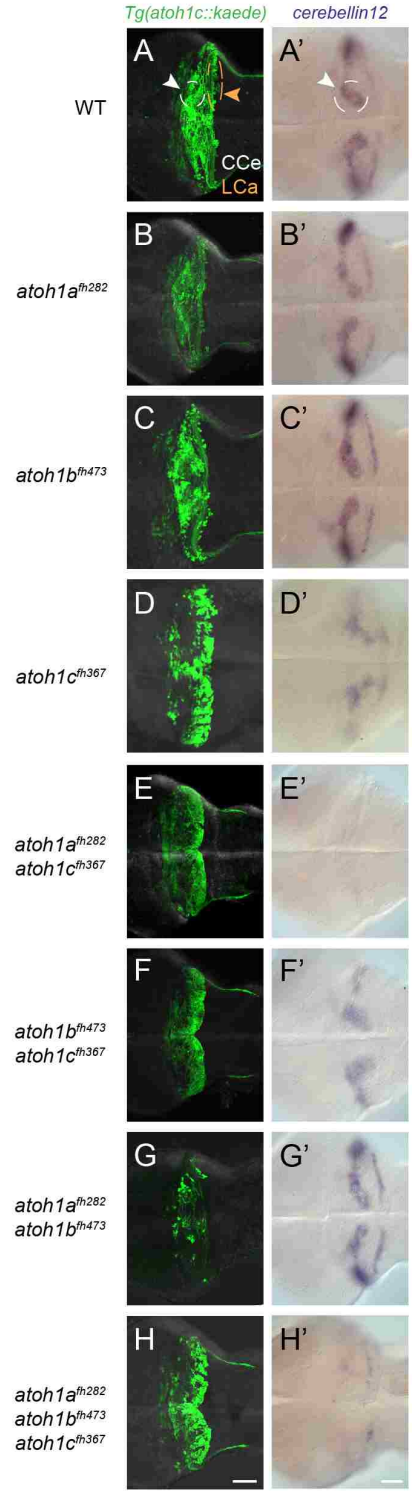

Figure 10. *atoh1a*, *atoh1b,* and *atoh1c* have non-overlapping roles in cerebellar development.

Images of 5 dpf wildtype (A), single (B-D), and compound (E-H) *atoh1* mutants with the *Tg(atoh1c:kaede)* (left column) or *cerebellin12* RNA *in situ* hybridization (right column). Dorsal views with anterior to the left. Scale bars: 50 uM.

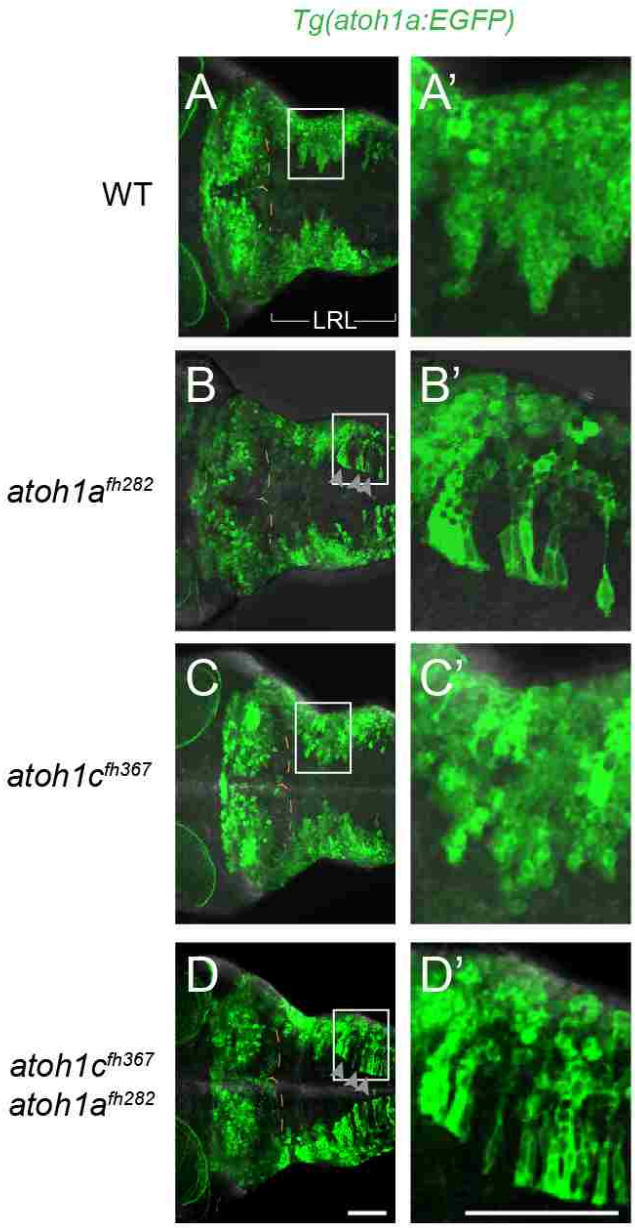

Figure 11. Atoh1a is required for delamination of neural progenitors in the lower rhombic lip (LRL).

Expression of *Tg(atoh1a:EGFP)* in wildtype (A), *atoh1a*^{fh282} (B), *atoh1c*^{fh367} (C), and *atoh1a*^{fh282}, *atoh1c*^{fh367} double mutants (D) at 5 dpf. Gray arrowheads indicate the apical surfaces of

progenitors that are retained at the LRL in *atoh1a* mutants. Orange dash line indicates URL; White bracket in A indicates LRL. Dorsal views with anterior to the left. Scale bar: 50 uM.

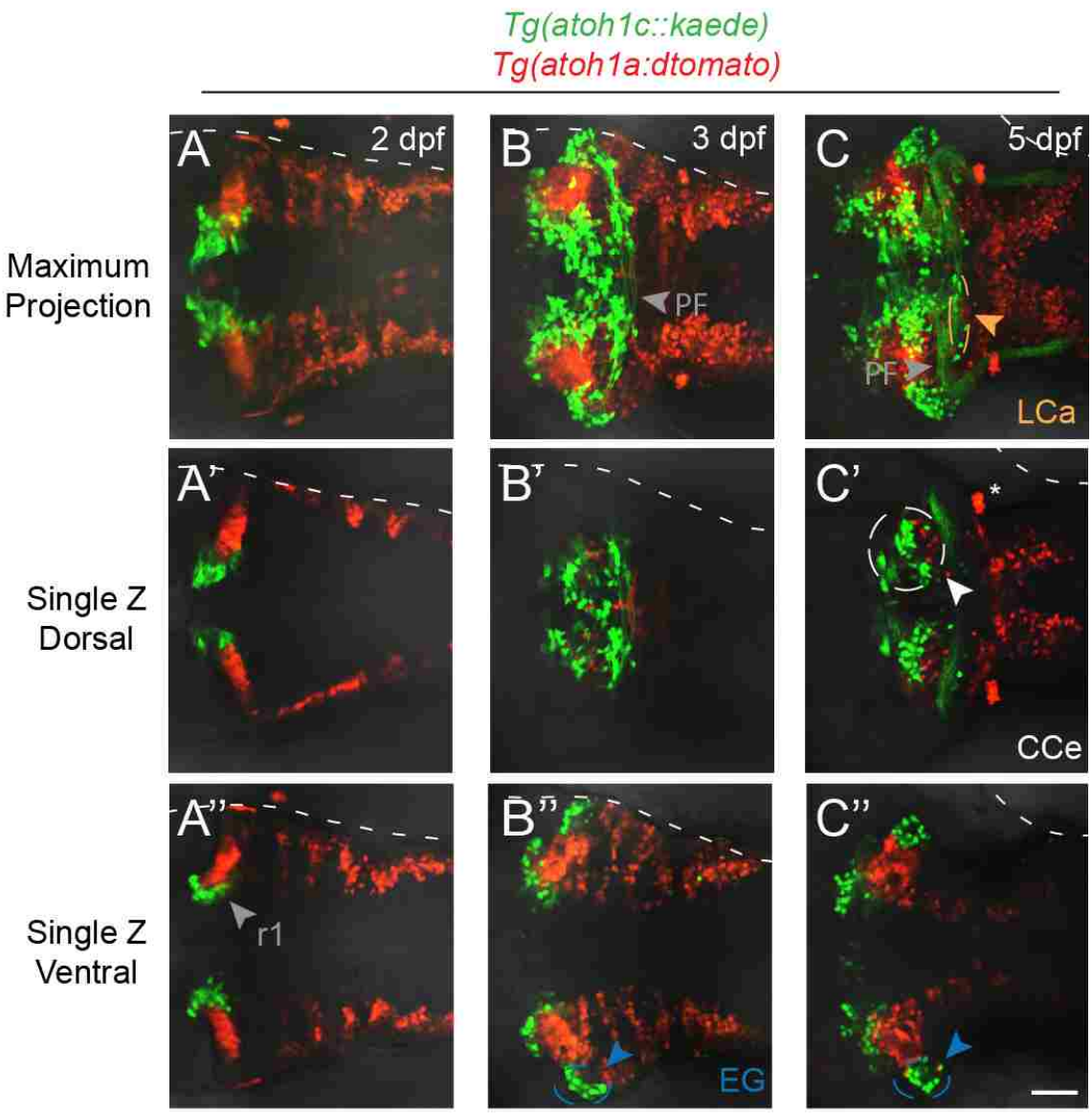

Figure 12. *atoh1a*- and *atoh1c*-derived neurons are not the same.

Live imaging of wildtype embryos with *Tg(atoh1c::kaede)* (green) and *Tg(atoh1a:dtomato)* (red) transgenes indicate *atoh1a* and *atoh1c*-derived neurons are distinct cerebellar populations and do not originate from a common progenitor pool. Maximum projections of a z-stack (A-C) and single z-slices at dorsal (A'-C') or ventral (A"-C") focal planes with anterior to the left. A: 2 dpf, B: 3 dpf, C: 5 dpf. Scale bar: 50 μM.

Chapter 5: Conclusions and Future Directions

Here we have defined the roles of *atoh1* genes in zebrafish cerebellar development with the use of live imaging of transgenic reporters combined with mutant analysis. We find that of *atoh1c* plays the most prominent role in the development of cerebellar granule neurons, both in the cerebellar corpus (CCe) and in the caudolateral lobes (EG and LCa). We show that *atoh1c* is required not for granule neuron specification per se, but for granule neuron progenitors to lose their epithelial character and migrate away from the upper rhombic lip and terminally differentiate. Finally, we show that *atoh1c* functions as an Wnt and Fgf "coincidence detector" at the mid-hindbrain boundary to specify an early population of neuronal progenitors that give rise to a ventral r1 neuron population related to the Locus Coeruleus which we hypothesize to be involved in arousal.

More *atoh1* Genes for More Granule Neuron Diversity

Lineage tracing experiments in mouse have shown that *atoh1*-expressing progenitors at the URL give rise sequentially to tegmental, deep cerebellar and cerebellar granule neurons (Fig. 12) (Machold and Fishell, 2005; Rose et al., 2009a; Wang et al., 2005). In this study, we have used the conserved cerebellar circuitry of the zebrafish to understand the role of the *atoh1* genes in specification of cerebellar neuronal populations. We consider granule neurons first. Based on *atoh1* expression patterns and lineage tracing of *atoh1a*+ cells in zebrafish which showed the presence of *atoh1a*-derived granule neurons in the Va and CCe but not the EG or LCa, Kani et al. predicted that *atoh1c and/or atoh1b* would be required for the specification of granule neuron populations in the EG and LCa. Our work confirms this prediction: zebrafish *atoh1c* is required

for the differentiation of EG and LCa granule neurons. Unexpectedly, however, *atoh1c* is also required for a population of granule neurons in the CCe that does not overlap with the *atoh1a* population, so that *atoh1c* and *atoh1a* together are required for the full complement of granule neurons in the CCe. Cerebellar granule neurons have been described as one singular population in vertebrates however our data suggests that the presence of additional *atoh1* genes has allowed for a previously undetected diversity in granule neurons within the CCe (Fig. 13), a homologous structure to the mammalian cerebellar vermis. Both populations express the mature granule neuron marker *cerebellin12*, and our overexpression experiment suggests that *atoh1a* can substitute for *atoh1c* in the *atoh1c*-derived population, so it is possible that the two populations function identically in the cerebellar circuit. However, in a recent RNA-Seq screen for granule neuron-specific genes, Takeuchi et al. (Takeuchi et al., 2016) identified several granule neuron markers that have distinct patterns of expression within the CCe, suggesting heterogeneity within granule neurons of the CCe.

Future studies will focus on determining whether these domains correspond to the *atoh1a* and *1c*-derived granule neurons by probing for differentially-expressed granule neuron markers in the *atoh1a* and *1c* single mutants. Defining the molecular signature of the *atoh1a* and *1*c-derived granule neurons will help us to better understand whether these populations have the same or different functions within the cerebellar circuit and could potentially reveal novel functions in zebrafish versus mouse granule neurons.

How do these individual populations contribute to the functional output of the cerebellum? The granule neurons that populate the EG and LCa are nearly depleted in the *atoh1c* mutant, therefore we can use the *atoh1c*^{fh367} larvae to understand the contribution of those granule neuron populations to vestibular-associated cerebellar behaviors, a function conserved in

mammals. Although we do not observe any gross behavioral defects in *atoh1c*^{fh367} mutants, using a specialized behavioral assay that measures the eye movements of larvae in response to a change in their body position, the vestibulo-ocular reflex (Mo et al., 2010), we would be able to detect vestibular-related defects in *atoh1c* mutant larvae behavior. We can also take advantage of other behavioral assays, such as those developed in the goldfish (Duran et al., 2014), to understand the function of granule neurons in navigation-based behavior. By using *atoh1a*^{fh282} and *atoh1c*^{fh367} double mutants, in which nearly all *cbln12*+ granule neurons are lost, we can determine the role of granule neurons in spatial cognition. We will take advantage of the compartmental nature of the zebrafish cerebellum to understand more about the functional contribution of regional populations of granule neurons to specific cerebellar-controlled behaviors.

MHB-derived *atoh1c* Neurons May Function in Arousal

We have identified a novel population of *atoh1c*-derived neurons closely associated with the Locus Coeruleus, an evolutionarily ancient noradrenergic population involved in states of arousal and sleep-wake cycles. Like the LC neurons, the *atoh1c* neurons are specified at the MHB in response to MHB-derived cues, migrate ventro-caudally into ventral r1, express tyrosine hydroxylase, and elaborate rostral, caudal, and cross-midline projections. However, unlike the LC, they do not express subsequent enzymes required for norepinephrine synthesis such as dopamine beta-hydroxylase (DBH; data not shown) and they turn off TH expression soon after arriving in ventral r1.

In addition to cerebellar granule neurons, lineage tracing in mouse has revealed an array of *atoh1*-derivatives including a number of tegmental pontine and deep cerebellar nuclei that

appear before granule precursors emerge from the URL (Fig. 13) (Machold and Fishell, 2005; Rose et al., 2009a; Wang et al., 2005). These include TH-positive cholinergic neurons in the lateral parabrachial and pedunculopontine tegmental nuclei, which lie adjacent to the Locus Coeruleus, are involved in arousal and attention, and have been implicated in the generation of REM sleep (Rose et al., 2009a). In a separate study, early-born *atoh1*-derived neurons in the peri-LC region were shown to regulate sleep states in mice (Hayashi et al., 2015). We hypothesize that the MHB population of LC-associated *atoh1c* neurons may play an ancient role in regulating states of arousal, possibly analogous to the lateral parabrachial or pedunculopontine tegmental nuclei. However, because these neurons persist in all *atoh1* mutant combinations we have generated, we are as yet unable to assess their functions in mutant fish. Interestingly, Machold and Fishell also noted that some *atoh1*-derived tegmental neurons are present in *atoh1* mouse mutants, suggesting the presence of compensating mechanisms for the specification of some Atoh1-derived neuronal populations in mouse as we have found in zebrafish.

Green et al. (Green et al., 2014) recently identified an early *atoh1* expression domain at the mid-hindbrain boundary in chick and mouse which arises in response to MHB signals independently of the URL *atoh1* expression domain and gives rise to early-born *atoh1* neurons in the tegmentum. Given the early onset of *atoh1c* expression at the MHB in zebrafish and its dependence on MHB-derived Wnt1 and Fgf signaling, it is likely that this domain, and its tegmental derivatives, are homologous to the tetrapod MHB *atoh1* population described by Green et al. Our finding that progenitors must be able to detect both Wnt and Fgf signals cell-autonomously to express *atoh1c* explains the progressive restriction of this progenitor zone to a single cell diameter from the MHB.

Future studies will focus on understanding more about the specification, connectivity, biochemical properties, and neuronal activity of this *atoh1c*+ r1 population. First, we will investigate which genes are required for specification of this population. We hypothesize that other bHLH transcription factors expressed at the MHB are compensating for the loss of *atoh1c* in the specification of the r1 neuron population. In order to determine if this is true, we will systematically knockout ubiquitously expressed E proteins, the obligate binding partners of tissue-specific bHLH transcription factors (Bertrand et al., 2002). E protein family members have been extensively studied in fly and mammals and their homologues have been identified in zebrafish (Wang et al., 2009). We can use CRISPR/Cas9 mutagenesis technology to knockdown members of the E protein gene family in the *atoh1c* MHB expression domain with the use of our *Tg(atoh1c:gal4ff)* driver crossed to a *Tg(UAS:cas9)* line. We will singly inject CRISPR guide RNA targeted against E protein genes and monitor the number and morphology of the r1 population using the *UAS:kaede* transgene present in the background of injected embryos. We would expect that the loss of E proteins, although only in a small population, would be detrimental to development of that region therefore we will screen for defects in the r1 population in the injected animals with mosaic knockdown, a method that has been shown to be effective in zebrafish (Shah et al., 2015). Once we determine whether a bHLH transcription factor family member is acting redundantly with *atoh1c* to specify the r1 neurons, we will query publicly available databases for bHLH genes that are expressed in the MHB region from 10 – 24 hpf to generate a candidate list of genes. After we have complied that list, we will use the same approached outlined above to determine which gene(s) is required for the specification of the *Tg(atoh1c::kaede)*+ r1 neurons.

Although we have characterized the location and gross connectivity patterns of the r1 neurons, in order to definitively identify our population in question more extensive characterization of its connections are necessary. Using a transsynaptic viral-based tracing method shown to be effective in zebrafish (Mundell et al., 2015), we will map all of the connections of *Tg(atoh1c::kaede)*+ r1 neurons. This will allow us to better understand its function and evolutionary relationship with neurons in the arousal circuit.

We have proposed that the *Tg(atoh1c::kaede)* r1 neurons are possibly analogous to the *atoh1*+ lateral parabrachial or pedunculopontine tegmental nuclei in mouse. Both of these nuclei contain neurons expressing a range of neurotransmitters. The lateral parabrachial nuclei contain glutamatergic, somatostatin, encephalin, corticotropin releasing hormone, and levodopa neurons and the pedunculopontine tegmental nuclei contain glutamatergic, corticotropin releasing hormone, nitric oxide, cholinergic, and levodopa neurons (Rose et al., 2009a). We will determine whether the *Tg(atoh1c::kaede)* neurons have a similar biochemical signature to either one of these populations with use of immunostaining and available transgenic zebrafish reporter lines.

Ultimately, we would like to understand how the neural activity of the r1 neurons effect behavior. Given the similarities and the close association of the *Tg(atoh1c::kaede)*+ neurons with the LC, we hypothesize that the r1 neurons function in the arousal circuit as well. The LC is activated in response to release of hypocretin (hcrt), a neuropeptide involved in maintaining wakefulness (Singh et al., 2015). Using a similar technique as Singh et al, we will test whether the *atoh1c*+ r1 neurons are also simulated in response to the activation of *hcrt*+ neurons and thus potentially involved in arousal. By generating a transgenic line containing *atoh1c:gal4ff, UAS:GCAMP6s,* and *hcrt:chR2* we will sequentially stimulate the hypocretin-releasing neurons and then monitor the activity of the *atoh1c*+ neurons with confocal imaging. In addition, we can

also test whether the LC and *Tg(atoh1c::kaede)+* neurons are functionally connected using a similar optogenetic approach. By crossing the *Tg(atoh1c::GCaMP6s)* to a LC-specific transgenic line such as *Tg(dbh:ChR2)*, we can test whether the *atoh1c+* neurons are stimulated in response to activation of the LC. We would be able to test if the reciprocal scenario is true as well by stimulating the *Tg(atoh1c::ChR2)+* neurons and monitoring the *Tg(dbh:GCaMP6)+* LC for subsequent activity. This would provide additional evidence of the close relationship between the LC and *Tg(atoh1c::kaede*) neurons and potentially clarify the role of the mouse lateral parabrachial or pedunculopontine tegmental nuclei in arousal.

atoh1 Genes and the Neuroepithelial Progenitor State

We have observed that in the absence of *atoh1c*, progenitors fail to migrate away from the URL and differentiate into granule neurons. Instead, *Tg(atoh1c::kaede)* cells accumulate at the URL in a post-mitotic, partially differentiated (NeuroD1-positive, HuC/D-negative) state. A similar accumulation of granule neuron progenitors at the URL was detected in mouse *atoh1* mutants (Ben-Arie et al., 1997; Ben-Arie et al., 2000). Our finding that non-migrated *atoh1c* mutant progenitors at the URL express NeuroD1 is interesting in light of the fact that in mice, granule neurons do not turn on NeuroD1 until after they complete their transit-amplifying divisions in the external granule cell layer (Miyata et al., 1999). The expression of NeuroD1 in undifferentiated granule neuron progenitors at the URL in *atoh1c* mutants may reflect the finding that most granule neurons in fish differentiate directly after leaving the URL, without going through a transit-amplifying phase (Butts et al., 2014; Chaplin et al., 2010).

Our high-resolution live imaging of these cells in *atoh1c* mutants shows that they exhibit a migratory behavior, extending dynamic basal processes similar to wildtype granule

progenitors. However, while wildtype granule progenitors are able to release their apical contacts and migrate away from the URL, *atoh1c* mutant cells cannot release their apical contacts and thus remain trapped at the URL. Recent studies have shown that eliminating N-cadherin-containing apical junctions is a critical step in neuronal differentiation (Matsuda et al., 2016; Pacary et al., 2012; Rousso et al., 2012). Interestingly, *atoh1c* mutant progenitors that escape the URL appear to complete differentiation and generate parallel fibers. We also noted that the morphology of the *atoh1a*^{fh282} cells in the LRL resemble that of *atoh1c*^{fh367} cells at the URL suggesting that a key function of *atoh1* genes may be to promote apical detachment of granule neuron progenitors, possibly by directly or indirectly repressing N-cadherin expression or activity.

Future studies will focus on further dissecting the role of *atoh1* genes in neuronal maturation. We speculate *atoh1* may promote the apical detachment of neural progenitors. In order to test this hypothesis, we will attempt to "override" the loss of Atoh1c in granule neuron progenitor by modulating N-Cadherin levels. It has recently been shown that reducing the levels of N-cadherin expression with a low-dose of an N-cadherin morpholino allows for delamination of neurons in *epb41l5*-deficient embryos (Matsuda et al., 2016). We will use a similar approach to attempt to "release" the granule neuron progenitors from the URL in the *atoh1c*^{fh367} cerebellum. Using our transgenic *atoh1c* reporter, we will be able to monitor the number of cells that migrate away from the URL. We predict that reducing levels of N-Cadherin will result in a much larger proportion of "escaper" cells in the *atoh1c*^{fh367} mutant compared to control morpholino injected siblings. In addition, we will use the same approach to attempt to rescue the *atoh1a*^{fh282} mutant LRL phenotype. If we are able to rescue the mutant phenotypes in one or both of these contexts that would provide additional evidence that the release of the apical attachment

in neural progenitors is a vital step in neuronal maturation and *atoh1* genes are essential in promoting this process.

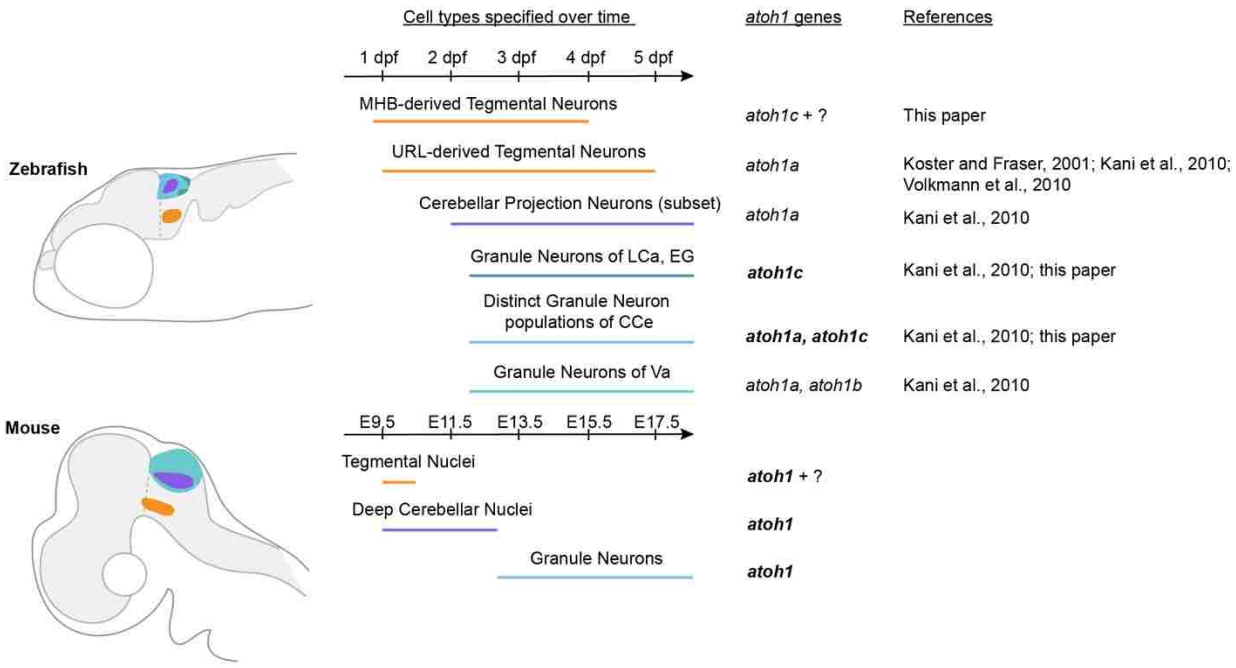

Figure 13. *atoh1*-derivates in zebrafish and mouse.

Schematic outlines *atoh1*-derivatives generated over time in the anterior hindbrain of zebrafish (top) and mouse (bottom). Bold text indicates gene has been shown to be required for development of the neuronal population. Homologous neuronal populations are indicated with the colored lines. Dpf: days post fertilization; E: embryonic day; CCe, corpus cerebelli; EG, eminentia granularis; LCa, lobus caudalis cerebelli; Va, valvula cerebelli.

Bibliography

Akazawa, C., Ishibashi, M., Shimizu, C., Nakanishi, S., Kageyama, R., 1995. A mammalian helix-loop-helix factor structurally related to the product of Drosophila proneural gene atonal is a positive transcriptional regulator expressed in the developing nervous system. The Journal of biological chemistry 270, 8730-8738.

Akitake, C.M., Macurak, M., Halpern, M.E., Goll, M.G., 2011. Transgenerational analysis of transcriptional silencing in zebrafish. Developmental biology 352, 191-201.

Altman, J., Bayer, S.A., 1997. Development of the cerebellar system : in relation to its evolution, structure, and functions. CRC Press, Boca Raton.

Ando, R., Hama, H., Yamamoto-Hino, M., Mizuno, H., Miyawaki, A., 2002. An optical marker based on the UV-induced green-to-red photoconversion of a fluorescent protein. Proceedings of the National Academy of Sciences of the United States of America 99, 12651-12656.

Artavanis-Tsakonas, S., Rand, M.D., Lake, R.J., 1999. Notch signaling: cell fate control and signal integration in development. Science 284, 770-776.

Bae, Y.K., Kani, S., Shimizu, T., Tanabe, K., Nojima, H., Kimura, Y., Higashijima, S., Hibi, M., 2009. Anatomy of zebrafish cerebellum and screen for mutations affecting its development. Developmental biology 330, 406-426.

Ben-Arie, N., Bellen, H.J., Armstrong, D.L., McCall, A.E., Gordadze, P.R., Guo, Q., Matzuk, M.M., Zoghbi, H.Y., 1997. Math1 is essential for genesis of cerebellar granule neurons. Nature 390, 169-172.

Ben-Arie, N., Hassan, B.A., Bermingham, N.A., Malicki, D.M., Armstrong, D., Matzuk, M., Bellen, H.J., Zoghbi, H.Y., 2000. Functional conservation of atonal and Math1 in the CNS and PNS. Development 127, 1039-1048.

Ben-Arie, N., McCall, A.E., Berkman, S., Eichele, G., Bellen, H.J., Zoghbi, H.Y., 1996. Evolutionary conservation of sequence and expression of the bHLH protein Atonal suggests a conserved role in neurogenesis. Hum Mol Genet 5, 1207-1216.

Bermingham, N.A., Hassan, B.A., Price, S.D., Vollrath, M.A., Ben-Arie, N., Eatock, R.A., Bellen, H.J., Lysakowski, A., Zoghbi, H.Y., 1999. Math1: an essential gene for the generation of inner ear hair cells. Science 284, 1837-1841.

Bermingham, N.A., Hassan, B.A., Wang, V.Y., Fernandez, M., Banfi, S., Bellen, H.J., Fritzsch, B., Zoghbi, H.Y., 2001. Proprioceptor pathway development is dependent on Math1. Neuron 30, 411-422.

Bertrand, N., Castro, D.S., Guillemot, F., 2002. Proneural genes and the specification of neural cell types. Nature reviews. Neuroscience 3, 517-530.

Bussmann, J., Schulte-Merker, S., 2011. Rapid BAC selection for tol2-mediated transgenesis in zebrafish. Development 138, 4327-4332.

Butts, T., Green, M.J., Wingate, R.J., 2014. Development of the cerebellum: simple steps to make a 'little brain'. Development 141, 4031-4041.

Caron, S.J., Prober, D., Choy, M., Schier, A.F., 2008. In vivo birthdating by BAPTISM reveals that trigeminal sensory neuron diversity depends on early neurogenesis. Development 135, 3259-3269.

Chaplin, N., Tendeng, C., Wingate, R.J., 2010. Absence of an external germinal layer in zebrafish and shark reveals a distinct, anamniote ground plan of cerebellum development. The Journal of neuroscience : the official journal of the Society for Neuroscience 30, 3048-3057.

Chiu, C.N., Prober, D.A., 2013. Regulation of zebrafish sleep and arousal states: current and prospective approaches. Front Neural Circuits 7, 58.

Davison, J.M., Akitake, C.M., Goll, M.G., Rhee, J.M., Gosse, N., Baier, H., Halpern, M.E., Leach, S.D., Parsons, M.J., 2007. Transactivation from Gal4-VP16 transgenic insertions for tissue-specific cell labeling and ablation in zebrafish. Developmental biology 304, 811-824.

Draper, B.W., McCallum, C.M., Stout, J.L., Slade, A.J., Moens, C.B., 2004. A high-throughput method for identifying N-ethyl-N-nitrosourea (ENU)-induced point mutations in zebrafish. Methods Cell Biol 77, 91-112.

Duran, E., Ocana, F.M., Martin-Monzon, I., Rodriguez, F., Salas, C., 2014. Cerebellum and spatial cognition in goldfish. Behav Brain Res 259, 1-8.

Englund, C., Kowalczyk, T., Daza, R.A., Dagan, A., Lau, C., Rose, M.F., Hevner, R.F., 2006. Unipolar brush cells of the cerebellum are produced in the rhombic lip and migrate through developing white matter. The Journal of neuroscience : the official journal of the Society for Neuroscience 26, 9184-9195.

Force, A., Lynch, M., Pickett, F.B., Amores, A., Yan, Y.L., Postlethwait, J., 1999. Preservation of duplicate genes by complementary, degenerative mutations. Genetics 151, 1531-1545.

Gazit, R., Krizhanovsky, V., Ben-Arie, N., 2004. Math1 controls cerebellar granule cell differentiation by regulating multiple components of the Notch signaling pathway. Development 131, 903-913.

Geling, A., Steiner, H., Willem, M., Bally-Cuif, L., Haass, C., 2002. A gamma-secretase inhibitor blocks Notch signaling in vivo and causes a severe neurogenic phenotype in zebrafish. EMBO reports 3, 688-694.

Godinho, L., Mumm, J.S., Williams, P.R., Schroeter, E.H., Koerber, A., Park, S.W., Leach, S.D., Wong, R.O., 2005. Targeting of amacrine cell neurites to appropriate synaptic laminae in the developing zebrafish retina. Development 132, 5069-5079.

Grant, P.K., Moens, C.B., 2010. The neuroepithelial basement membrane serves as a boundary and a substrate for neuron migration in the zebrafish hindbrain. Neural development 5, 9.

Gray, P.A., 2008. Transcription factors and the genetic organization of brain stem respiratory neurons. J Appl Physiol (1985) 104, 1513-1521.

Green, M.J., Myat, A.M., Emmenegger, B.A., Wechsler-Reya, R.J., Wilson, L.J., Wingate, R.J., 2014. Independently specified Atoh1 domains define novel developmental compartments in rhombomere 1. Development 141, 389-398.

Guo, S., Brush, J., Teraoka, H., Goddard, A., Wilson, S.W., Mullins, M.C., Rosenthal, A., 1999. Development of noradrenergic neurons in the zebrafish hindbrain requires BMP, FGF8, and the homeodomain protein soulless/Phox2a. Neuron 24, 555-566.

Hartenstein, A.Y., Rugendorff, A., Tepass, U., Hartenstein, V., 1992. The function of the neurogenic genes during epithelial development in the Drosophila embryo. Development 116, 1203-1220.

Hashimoto, M., Hibi, M., 2012. Development and evolution of cerebellar neural circuits. Development, growth & differentiation 54, 373-389.

Hayashi, Y., Kashiwagi, M., Yasuda, K., Ando, R., Kanuka, M., Sakai, K., Itohara, S., 2015. Cells of a common developmental origin regulate REM/non-REM sleep and wakefulness in mice. Science 350, 957-961.

Helms, A.W., Johnson, J.E., 1998. Progenitors of dorsal commissural interneurons are defined by MATH1 expression. Development 125, 919-928.

Hibi, M., Shimizu, T., 2012. Development of the cerebellum and cerebellar neural circuits. Developmental neurobiology 72, 282-301.

Jarman, A.P., Grau, Y., Jan, L.Y., Jan, Y.N., 1993. atonal is a proneural gene that directs chordotonal organ formation in the Drosophila peripheral nervous system. Cell 73, 1307-1321.

Jarman, A.P., Grell, E.H., Ackerman, L., Jan, L.Y., Jan, Y.N., 1994. Atonal is the proneural gene for Drosophila photoreceptors. Nature 369, 398-400.

Jarman, A.P., Sun, Y., Jan, L.Y., Jan, Y.N., 1995. Role of the proneural gene, atonal, in formation of Drosophila chordotonal organs and photoreceptors. Development 121, 2019-2030.

Kani, S., Bae, Y.K., Shimizu, T., Tanabe, K., Satou, C., Parsons, M.J., Scott, E., Higashijima, S., Hibi, M., 2010. Proneural gene-linked neurogenesis in zebrafish cerebellum. Developmental biology 343, 1-17.

Kaslin, J., Ganz, J., Geffarth, M., Grandel, H., Hans, S., Brand, M., 2009. Stem cells in the adult zebrafish cerebellum: initiation and maintenance of a novel stem cell niche. The Journal of neuroscience : the official journal of the Society for Neuroscience 29, 6142-6153.

Kemp, H.A., Carmany-Rampey, A., Moens, C., 2009. Generating chimeric zebrafish embryos by transplantation. J Vis Exp.

Kim, C.H., Ueshima, E., Muraoka, O., Tanaka, H., Yeo, S.Y., Huh, T.L., Miki, N., 1996. Zebrafish elav/HuC homologue as a very early neuronal marker. Neurosci Lett 216, 109-112.

Kimmel, C.B., Ballard, W.W., Kimmel, S.R., Ullmann, B., Schilling, T.F., 1995. Stages of embryonic development of the zebrafish. Developmental dynamics : an official publication of the American Association of Anatomists 203, 253-310.

Koster, R.W., Fraser, S.E., 2001. Direct imaging of in vivo neuronal migration in the developing cerebellum. Current biology : CB 11, 1858-1863.

Lee, Y., Grill, S., Sanchez, A., Murphy-Ryan, M., Poss, K.D., 2005. Fgf signaling instructs position-dependent growth rate during zebrafish fin regeneration. Development 132, 5173-5183.

Leto, K., Arancillo, M., Becker, E.B., Buffo, A., Chiang, C., Ding, B., Dobyns, W.B., Dusart, I., Haldipur, P., Hatten, M.E., Hoshino, M., Joyner, A.L., Kano, M., Kilpatrick, D.L., Koibuchi, N., Marino, S., Martinez, S., Millen, K.J., Millner, T.O., Miyata, T., Parmigiani, E., Schilling, K., Sekerkova, G., Sillitoe, R.V., Sotelo, C., Uesaka, N., Wefers, A., Wingate, R.J., Hawkes, R., 2015. Consensus Paper: Cerebellar Development. Cerebellum.

Machold, R., Fishell, G., 2005. Math1 is expressed in temporally discrete pools of cerebellar rhombic-lip neural progenitors. Neuron 48, 17-24.

Machold, R.P., Kittell, D.J., Fishell, G.J., 2007. Antagonism between Notch and bone morphogenetic protein receptor signaling regulates neurogenesis in the cerebellar rhombic lip. Neural development 2, 5.

Martin, B.L., Kimelman, D., 2012. Canonical Wnt signaling dynamically controls multiple stem cell fate decisions during vertebrate body formation. Developmental cell 22, 223-232.

Matsuda, M., Rand, K., Palardy, G., Shimizu, N., Ikeda, H., Dalle Nogare, D., Itoh, M., Chitnis, A.B., 2016. Epb41l5 competes with Delta as a substrate for Mib1 to coordinate specification and differentiation of neurons. Development 143, 3085-3096.

Matsui, H., Namikawa, K., Babaryka, A., Koster, R.W., 2014. Functional regionalization of the teleost cerebellum analyzed in vivo. Proceedings of the National Academy of Sciences of the United States of America 111, 11846-11851.

Millimaki, B.B., Sweet, E.M., Dhason, M.S., Riley, B.B., 2007. Zebrafish atoh1 genes: classic proneural activity in the inner ear and regulation by Fgf and Notch. Development 134, 295-305.

Miyata, T., Maeda, T., Lee, J.E., 1999. NeuroD is required for differentiation of the granule cells in the cerebellum and hippocampus. Genes & development 13, 1647-1652.

Mo, W., Chen, F., Nechiporuk, A., Nicolson, T., 2010. Quantification of vestibular-induced eye movements in zebrafish larvae. BMC Neurosci 11, 110.

Mundell, N.A., Beier, K.T., Pan, Y.A., Lapan, S.W., Goz Ayturk, D., Berezovskii, V.K., Wark, A.R., Drokhlyansky, E., Bielecki, J., Born, R.T., Schier, A.F., Cepko, C.L., 2015. Vesicular stomatitis virus enables gene transfer and transsynaptic tracing in a wide range of organisms. The Journal of comparative neurology 523, 1639-1663.

Pacary, E., Martynoga, B., Guillemot, F., 2012. Crucial first steps: the transcriptional control of neuron delamination. Neuron 74, 209-211.

Pujol-Marti, J., Zecca, A., Baudoin, J.P., Faucherre, A., Asakawa, K., Kawakami, K., Lopez-Schier, H., 2012. Neuronal birth order identifies a dimorphic sensorineural map. The Journal of neuroscience : the official journal of the Society for Neuroscience 32, 2976-2987.

Rhinn, M., Brand, M., 2001. The midbrain--hindbrain boundary organizer. Current opinion in neurobiology 11, 34-42.

Rose, M.F., Ahmad, K.A., Thaller, C., Zoghbi, H.Y., 2009a. Excitatory neurons of the proprioceptive, interoceptive, and arousal hindbrain networks share a developmental requirement for Math1. Proceedings of the National Academy of Sciences of the United States of America 106, 22462-22467.

Rose, M.F., Ren, J., Ahmad, K.A., Chao, H.T., Klisch, T.J., Flora, A., Greer, J.J., Zoghbi, H.Y., 2009b. Math1 is essential for the development of hindbrain neurons critical for perinatal breathing. Neuron 64, 341-354.

Rousso, D.L., Pearson, C.A., Gaber, Z.B., Miquelajauregui, A., Li, S., Portera-Cailliau, C., Morrisey, E.E., Novitch, B.G., 2012. Foxp-mediated suppression of N-cadherin regulates neuroepithelial character and progenitor maintenance in the CNS. Neuron 74, 314-330.

Sanjana, N.E., Cong, L., Zhou, Y., Cunniff, M.M., Feng, G., Zhang, F., 2012. A transcription activator-like effector toolbox for genome engineering. Nature protocols 7, 171-192.

Scott, E.K., Mason, L., Arrenberg, A.B., Ziv, L., Gosse, N.J., Xiao, T., Chi, N.C., Asakawa, K., Kawakami, K., Baier, H., 2007. Targeting neural circuitry in zebrafish using GAL4 enhancer trapping. Nature methods 4, 323-326.

Shah, A.N., Davey, C.F., Whitebirch, A.C., Miller, A.C., Moens, C.B., 2015. Rapid reverse genetic screening using CRISPR in zebrafish. Nat Methods 12, 535-540.

Singh, C., Oikonomou, G., Prober, D.A., 2015. Norepinephrine is required to promote wakefulness and for hypocretin-induced arousal in zebrafish. Elife 4, e07000.

Takeuchi, M., Matsuda, K., Yamaguchi, S., Asakawa, K., Miyasaka, N., Lal, P., Yoshihara, Y., Koga, A., Kawakami, K., Shimizu, T., Hibi, M., 2015a. Establishment of Gal4 transgenic zebrafish lines for analysis of development of cerebellar neural circuitry. Developmental biology 397, 1-17.

Takeuchi, M., Yamaguchi, S., Sakakibara, Y., Hayashi, T., Matsuda, K., Hara, Y., Tanegashima, C., Shimizu, T., Kuraku, S., Hibi, M., 2016. Gene expression profiling of granule cells and Purkinje cells in the zebrafish cerebellum. The Journal of comparative neurology.

Takeuchi, M., Yamaguchi, S., Yonemura, S., Kakiguchi, K., Sato, Y., Higashiyama, T., Shimizu, T., Hibi, M., 2015b. Type IV Collagen Controls the Axogenesis of Cerebellar Granule Cells by Regulating Basement Membrane Integrity in Zebrafish. PLoS genetics 11, e1005587.

Thisse, C., Thisse, B., Schilling, T.F., Postlethwait, J.H., 1993. Structure of the zebrafish snail1 gene and its expression in wild-type, spadetail and no tail mutant embryos. Development 119, 1203-1215.

Volkmann, K., Chen, Y.Y., Harris, M.P., Wullimann, M.F., Koster, R.W., 2010. The zebrafish cerebellar upper rhombic lip generates tegmental hindbrain nuclei by long-distance migration in an evolutionary conserved manner. The Journal of comparative neurology 518, 2794-2817.

Volkmann, K., Rieger, S., Babaryka, A., Koster, R.W., 2008. The zebrafish cerebellar rhombic lip is spatially patterned in producing granule cell populations of different functional compartments. Developmental biology 313, 167-180.

Wada, H., Ghysen, A., Satou, C., Higashijima, S., Kawakami, K., Hamaguchi, S., Sakaizumi, M., 2010. Dermal morphogenesis controls lateral line patterning during postembryonic development of teleost fish. Developmental biology 340, 583-594.

Wang, V.Y., Rose, M.F., Zoghbi, H.Y., 2005. Math1 expression redefines the rhombic lip derivatives and reveals novel lineages within the brainstem and cerebellum. Neuron 48, 31-43.

Wang, Y., Chen, K., Yao, Q., Zheng, X., Yang, Z., 2009. Phylogenetic analysis of zebrafish basic helix-loop-helix transcription factors. J Mol Evol 68, 629-640.

Wingate, R.J., Hatten, M.E., 1999. The role of the rhombic lip in avian cerebellum development. Development 126, 4395-4404.